Synthesis, spectroscopic characterization, and structural studies of organogermanium tri- and monothiocarbonates. Crystal structures of $Me_2Ge[S_2CSEt]_2$, $Ph_3Ge[SCO_2Me]$, $Ph_3Ge[SCO_2(\textit{i}\text{-Pr})]$, and $Ph_2Ge[SCO_2Me]_2$

John E. Drake and Jincai Yang

Abstract: Two series of *S*-alkyl trithiocarbonate derivatives of dimethylgermane, $Me_2Ge[S_2CSR]_2$, and halodiphenylgermane, $Ph_2GeX[S_2CSR]$, where R = Me, *i*-Pr, *n*-Pr, *n*-Bu and X = Cl, Br, and three series of *O*-alkyl monothiocarbonate derivatives of triphenylgermane, $Ph_3Ge[SCO_2R]$, diphenylgermane, $Ph_2Ge[SCO_2R]$, and trimethylgermane, $Me_3Ge[SCO_2R]$, where R = Me, *i*-Pr, and *n*-Pr, have been prepared in 73–92% yields by the reaction of the potassium or sodium salt of the appropriate tri- or monothiocarbonic acid with dichlorodimethyl-, chlorotriphenyl-, dichlorodiphenyl-, and chlorotrimethylgermane. The compounds were principally characterized by infrared, Raman, and ^1H and ^{13}C NMR spectroscopy, including some variable temperature studies, as well as by mass spectrometry. $Me_2Ge[S_2CSEt]_2$, **1**: $P2_1/m$ (No. 11) with cell parameters $a = 6.647(4)$ Å, $b = 7.423(2)$ Å, $c = 16.290(4)$ Å, $\beta = 91.07(3)°$, $V = 803.6(4)$ Å^3, $Z = 2$, $R = 0.0484$, $R_w = 0.0485$. $Ph_3Ge[SCO_2Me]$, **13**: $P\bar{1}$ (No. 2) with cell parameters $a = 9.970(4)$ Å, $b = 10.660(3)$ Å, $c = 9.853(2)$ Å, $\alpha = 101.78(2)°$, $\beta = 109.98(2)°$, $\gamma = 89.76(3)°$, $V = 961.0(5)$ Å^3, $Z = 2$, $R = 0.0534$, $R_w = 0.0451$. $Ph_3Ge[SCO_2(\textit{i}\text{-Pr})]$, **14**: $P\bar{1}$ (No. 2) with cell parameters $a = 14.386(7)$ Å, $b = 18.598(6)$ Å, $c = 9.223(3)$ Å, $\alpha = 102.85(3)°$, $\beta = 94.58(3)°$, $\gamma = 108.13(3)°$, $V = 2256(1)$ Å^3, $Z = 2$, $R = 0.0545$, $R_w = 0.0552$. $Ph_2Ge[SCO_2Me]_2$, **16**: Cc, (No. 9) with cell parameters $a = 11.790(4)$ Å, $b = 13.696(5)$ Å, $c = 23.232(6)$ Å, $\beta = 92.26(3)°$, $V = 3748(2)$ Å^3, $Z = 8$, $R = 0.0563$, $R_w = 0.0512$. The immediate environment about Ge is that of tetrahedral but the orientations of the thiocarbonate groups display interesting features.

Key words: structure, germanium, phenyl, methyl, thiocarbonates.

Résumé : On a préparé deux séries de dérivés trithiocarbonates de *S*-alkyle du diméthylgermane, $Me_2Ge[S_2CSR]_2$, et d'halogénodiphénylgermane, $Ph_2GeX[S_2CSR]$, dans lesquels R = Me, *i*-Pr, Pr, Bu et X = Cl, Br et trois séries de dérivés monothiocarbonates de *O*-alkyle du triphénylgermane, $Ph_3Ge[SCO_2R]$, du diphénylgermane, $Ph_2Ge[SCO_2R]$, et du triméthylgermane, $Me_3Ge[SCO_2R]$, dans lesquels R = Me, *i*-Pr et Pr, avec des rendements allant de 73 à 92% en procédant à la réaction du sel de sodium ou de potassium de l'acide tri- ou monothiocarbonique approprié avec le dichlorodiméthyl-, chlorotriphényl-, dichlorodiphényl- et le chlorotriméthylgermane. On a généralement caractérisé les composés par le biais des spectroscopies infrarouge, Raman et RMN du ^1H et du ^{13}C, y compris des études à températures variables, ainsi que par spectrométrie de masse. $Me_2Ge[S_2CSEt]_2$, **1** : $P2_1/m$ (No. 11), avec $a = 6{,}647(4)$, $b = 7{,}423(2)$ et $c = 16{,}290(4)$ Å, $\beta = 91{,}07(3)°$, $V = 803{,}6(4)$ Å^3, $Z = 2$, $R = 0{,}0484$, $R_w = 0{,}0485$. $Ph_3Ge[SCO_2Me]$, **13** : $P\bar{1}$ (No. 2), avec $a = 9{,}970(4)$, $b = 10{,}660(3)$ et $c = 9{,}853(2)$ Å, $\alpha = 101{,}78(2)°$, $\beta = 109{,}98(2)°$ et $\gamma = 89{,}76(3)°$, $V = 961{,}0(5)$ Å^3, $Z = 2$, $R = 0{,}0534$, $R_w = 0{,}0451$. $Ph_3Ge[SCO_2(\textit{i}\text{-Pr})]$, **14** :$P\bar{1}$ (No. 2), avec $a = 14{,}386(7)$, $b = 18{,}598(6)$ et $c = 9{,}223(3)$ Å, $\alpha = 102{,}85(3)°$, $\beta = 94{,}58(3)°$ et $\gamma = 108{,}13(3)°$, $V = 2256(1)$ Å^3, $Z = 2$, $R = 0{,}0545$, $R_w = 0{,}0552$. $Ph_2Ge[SCO_2Me]_2$, **16** : Cc (No. 9), avec $a = 11{,}790(4)$, $b = 13{,}696(5)$ et $c = 23{,}232(6)$ Å, $\beta = 92{,}26(3)°$, $V = 3748(2)$ Å^3, $Z = 8$, $R = 0{,}0563$, $R_w = 0{,}0512$. L'environnement immédiat du Ge est tétraédrique, mais les orientations des groupes thiocarbonates présentent des caractéristiques intéressantes.

Mots clés : structure, germanium, phényle, méthyle, thiocarbonates.

[Traduit par la rédaction]

Introduction

A wide variety of studies on *O*-alkyl dithiocarbonates (xanthates) have been reported but the analogous trithio- and monothiocarbonates have received considerably less attention. For trithiocarbonates, this can be attributed to the relative ease with which they undergo carbon disulfide elimination (1–3) and most reports relate to transition metal derivatives. As part of our studies on organogermanium dithio carbonates, carbamates, and phosphates (4–14), we have reported on a few

Received October 3, 1997.

J.E. Drake[1] and J. Yang.[2] Department of Chemistry and Biochemistry, University of Windsor, Windsor, ON N9B 3P4, Canada.

[1] Author to whom correspondence may be addressed. Telephone: (519) 253-4232, ext 3551. Fax: (519) 973-7098.

Can. J. Chem. **76**: 319–334 (1998)

trithiocarbonate derivatives (15), and herein is reported an extension of this work involving *S*-alkyl trithiocarbonate derivatives of dimethylgermane, $Me_2Ge[S_2CSR]_2$, and halodiphenylgermane, $Ph_2GeX[S_2CSR]$, where R = Me, *i*-Pr, *n*-Pr, *n*-Bu and X = Cl, Br. Monothiocarbonate derivatives have received even less attention and again virtually all reports have involved transition metal complexes (16–20). With the exception of those on alkali metal salts (21), only one report on main group element monothiocarbonates, describing some organotellurium derivatives, has appeared (22). Three series of *O*-alkyl monothiocarbonate derivatives of triphenylgermane, $Ph_3Ge[SCO_2R]$, diphenylgermane, $Ph_2Ge[SCO_2R]_2$, and trimethylgermane, $Me_3Ge[SCO_2R]$, where R = Me, *i*-Pr, and *n*-Pr are discussed. All of the compounds described were characterized by NMR, infrared, and Raman spectroscopy, as well as by X-ray crystallography when suitable crystals were obtained.

Experimental

Materials

Me_3GeCl, Me_2GeCl_2, Ph_3GeCl, Ph_2GeCl_2, and Me_3SiBr were obtained from Aldrich and Strem Chemicals, all starting materials being used as supplied. All solvents were dried and distilled prior to use and all reactions were carried out under anhydrous conditions. The salts KS_2CSR, where R = Et, *i*-Pr, *n*-Pr, *n*-Bu, were prepared as described earlier (15) and were further purified by a method based on that described for dithiocarbonates (23). The salts $NaSCO_2R$, where R = Me, *i*-Pr, *n*-Pr, were prepared as follows. Typically, sodium metal (ca. 1.0 g) was added to dry *i*-PrOH (ca. 10 mL) in a flask under N_2 gas and the reaction allowed to proceed for 1 h, before COS gas was bubbled in for 10 min. This was followed by distillation under vacuum and pumping to dryness to give $NaSCO_2(i\text{-Pr})$; 5.5 g, yield 89%. IR (cm^{-1}), main features: 1550 br s, 1384 mw, 1371 m, 1186 s, 1086 br s, 973 m, 688 m; Raman (cm^{-1}): 830 (100); ^1H NMR (ppm relative to DSS): 4.83 (OC*H*, septet, 6.34 Hz), 1.21 ($OCCH_3$, d, 6.34 Hz); ^{13}C NMR (ppm relative to DSS): 71.12 (O*C*), 21.98 (OC*C*), 185.86 (SCO_2). Similarly were prepared $NaSCO_2Me$; yield 85%. IR (cm^{-1}), main features: 1592 vs, vbr, 1428 m, 1188 m, 1120 vs, br, 1040 m, 965 mw, 695 mw; Raman (cm^{-1}): 825 (100): ^1H NMR (ppm relative to DSS): 3.68 (CH_3), ^{13}C NMR (ppm relative to DSS): 54.36 (CH_3), 186.89 (SCO_2), and $NaSCO_2(n\text{-Pr})$; yield 92%. IR (cm^{-1}) main features: 1614 vs, br, 1432 s, 1136 s, 1098 s, 1000 m, 827 m, 668 ms; Raman (cm^{-1}): 841 (100); ^1H NMR (ppm relative to DSS): 4.01 (OCH_2, triplet, 6.6 Hz), 1.65 ($OCCH_2$, m), 0.94 (CH_3, triplet, 7.4 Hz); ^{13}C NMR (ppm relative to DSS): 69.34 (O*C*), 22.63(OC*C*), 10.66 (OCC*C*), 186.64 (SCO_2).

Synthesis of (*S*-organo trithiocarbonato) dimethylgermanes

$Me_2Ge[S_2CSEt]_2$, **1**, *$Me_2Ge[S_2CS(i\text{-Pr})]_2$,* **2**, *$Me_2Ge[S_2CS(n\text{-Pr})]_2$,* **3**, *and $Me_2Ge[S_2CS(n\text{-Bu})]_2$,* **4**

Typically, Me_2GeCl_2 (0.10 mL, 0.87 mmol) and dried CS_2 (ca. 10 mL) were distilled onto previously degassed KS_2CSEt (0.35 g, 1.99 mmol) in a flask held at –196°C. The contents were stirred for ca. 4 h at 0°C. Unreacted KS_2CSEt and KCl were filtered off and solvent allowed to evaporate under vacuum to produce $Me_2Ge[S_2CSEt]_2$, **1**, a yellow solid (0.30 g, 0.80 mmol, yield 92%). Recrystallization from CS_2 at –15°C gave yellow crystals, mp 35°C. Prepared similarly were $Me_2Ge[S_2CS(i\text{-Pr})]_2$, **2**, $Me_2Ge[S_2CS(n\text{-Pr})]_2$, **3**, and $Me_2Ge[S_2CS(n\text{-Bu})]_2$, **4**, all as yellow oils in yields of 82, 85, and 80%, respectively.

Synthesis of (*S*-organo trithiocarbonato)chlorodimethylgermanes

$Ph_2GeCl[S_2CSEt]$, **5**, *$Ph_2GeCl[S_2CS(i\text{-Pr})]$,* **6**, *$Ph_2GeCl[S_2CS(n\text{-Pr})]$,* **7**, *$Ph_2GeCl[S_2CS(n\text{-Bu})]$,* **8**

Typically, Ph_2GeCl_2 (0.30 g, 1.02 mmol), which was contained in a small vial, and dried KS_2CSEt (0.18 g, 1.02 mmol) were placed in a flask, which was then cooled to –196°C, degassed, and dried CS_2 (ca. 8 mL) was distilled in. The mixture was stirred for ca. 2 h at 0°C, KS_2CSEt and KCl filtered off, and the solvent allowed to evaporate under vacuum to produce $Ph_2GeCl[S_2CSEt]$, **5**, a yellow oil (0.32 g, 0.81 mmol, yield 80%). Prepared similarly were $Ph_2GeCl[S_2CS(i\text{-Pr})]$, **6**, $Ph_2GeCl[S_2CS(n\text{-Pr})]$, **7**, and $Ph_2GeCl[S_2CS(n\text{-Bu})]$, **8**, all as yellow oils with yields of 80, 78, and 84%, respectively.

Synthesis of (*S*-organo trithiocarbonato)bromodimethylgermanes

$Ph_2GeBr[S_2CSEt]$, **9**, *$Ph_2GeBr[S_2CS(i\text{-Pr})]$,* **10**, *$Ph_2GeBr[S_2CS(n\text{-Pr})]$,* **11**, *and $Ph_2GeBr[S_2CS(n\text{-Bu})]$,* **12**

Typically, $Ph_2GeCl[S_2CSEt]$ was prepared in situ as above from Ph_2GeCl_2 (0.31 g, 1.05 mmol) and dried KS_2CSEt (0.18 g, 1.05 mmol). The flask was recooled to –196°C, degassed again, Me_3SiBr (ca. 0.3 mL) was distilled in, and then the mixture was stirred for 2 h at 0°C, followed by evaporation under vacuum to remove Me_3SiCl and any unreacted Me_3SiBr, to produce $Ph_2GeBr[S_2CSEt]$, **9**, as a yellow oil (0.39 g, 0.88 mmol, yield 84%). Similarly were prepared $Ph_2GeBr[S_2CS(i\text{-Pr})]$, **10**, $Ph_2GeBr[S_2CS(n\text{-Pr})]$, **11**, and $Ph_2GeBr[S_2CS(n\text{-Bu})]$, **12**, all as yellow oils in yields of 83, 80, and 88%, respectively. Crystallization of **2**–**12** using a variety of solvents and solvent mixtures was not successful, and attempts at obtaining boiling points resulted in the immediate release of CS_2.

Attempted preparations of halodimethylgermanium trithiocarbonates

Efforts to synthesize the species Me_2GeClL and Me_2GeBrL, where $L = S_2CSR$; R = Et, *i*-Pr, *n*-Pr, *n*-Bu, were not successful. The appropriate stoichiometric reactions were shown by NMR spectroscopy to always give mixtures of Me_2GeXL and Me_2GeL_2. Because of the lack of stability of these compounds, isolation by column chromatography did not give the desired compounds but only decomposition products consistent with CS_2 elimination.

Synthesis of (*O*-organo monothiocarbonato)-triphenylgermanes

$Ph_3Ge[SCO_2Me]$, **13**, *$Ph_3Ge[SCO_2(i\text{-Pr})]$,* **14**, *and $Ph_3Ge[SCO_2(n\text{-Pr})]$,* **15**

Typically, Ph_3GeCl (0.25 g, 0.74 mmol) and excess, dried $NaSCO_2Me$ (0.09 g, 0.79 mmol) were placed in a previously evacuated flask and CH_2Cl_2 (ca. 15 mL) was distilled in at

–196°C. The mixture was stirred for 4 h at room temperature, followed by filtration and evaporation under vacuum to give Ph$_3$Ge[SCO$_2$Me], **13**, a colorless solid (0.26 g, 0.66 mmol, yield 89%). Recrystallization from a CH$_2$Cl$_2$–*n*-hexane mixture gave colorless crystals, mp 101–102°C. Peaks corresponding to ^{74}Ge in a typical germanium cluster were seen at *m/z* (relative intensity): 396 ((M)$^+$, 2%), 337 ((M – CO$_2$Me)$^+$, 3%), 319 ((M – Ph)$^+$, 10%), 305 ((M – SCO$_2$Me)$^+$, 100%), 259 ((M – PhCO$_2$Me)$^+$, 30%), 228 ((M – PhSCO$_2$Me)$^+$, 30%), 183 ((M – Ph$_2$CO$_2$Me)$^+$, 5%), and 151 ((M – Ph$_2$SCO$_2$Me)$^+$, 50%). Prepared similarly was Ph$_3$Ge[SCO$_2$(*i*-Pr)], **14**, a colorless solid (0.30 g, 0.71 mmol, yield 86%). Recrystallization from a CH$_2$Cl$_2$–*n*-hexane mixture gave colorless crystals, mp 98–99°C. Similarly was prepared Ph$_3$Ge[SCO$_2$(*n*-Pr)], **15**, a colorless solid (0.29 g, 0.69 mmol, yield 89%), mp 91–93°C. Peaks corresponding to ^{74}Ge were seen at *m/z* (relative intensity): 305 ((M – SCO$_2$C$_3$H$_7$)$^+$, 100%), 287 ((M – PhSCO)$^+$, 15%), 245 ((M – PhSCOC$_3$H$_6$)$^+$, 20%), 228 ((M – PhSCO$_2$C$_3$H$_7$)$^+$, 38%), and 151 ((M – Ph$_2$SCO$_2$C$_3$H$_7$)$^+$, 46%). However, attempts at recrystallization failed to give crystals suitable for X-ray diffraction.

Synthesis of bis(*O*-organo monothiocarbonato)-diphenylgermanes

Ph$_2$Ge[SCO$_2$Me]$_2$, **16***, Ph$_2$Ge[SCO$_2$(i-Pr)]$_2$,* **17***, and Ph$_2$Ge[SCO$_2$(*n*-Pr)]$_2$,* **18**

Typically, Ph$_2$GeCl$_2$ (0.25 g, 0.85 mmol) in a vial and NaSCO$_2$Me (0.25 g, 2.19 mmol) were placed in a flask and CH$_2$Cl$_2$ (ca. 15 mL) was distilled in at –196°C. Reaction and separation were carried out as for **13** to give Ph$_2$Ge[SCO$_2$Me]$_2$, **16**, as a colorless solid (0.30 g, 0.70 mmol, yield 82%). Recrystallization from a CH$_2$Cl$_2$–*n*-hexane mixture gave colorless crystals, mp 69°C. Peaks corresponding to ^{74}Ge were seen at *m/z* (relative intensity): 351 ((M – CO$_2$Me)$^+$, 1%), 319 ((M – SCO$_2$Me)$^+$, 8%), 259 ((M – SCO$_2$Me(CO$_2$Me))$^+$, 80%), 229 ((M – SCO$_2$Me(SCO$_2$CH$_2$))$^+$, 60%), 151 ((M – Ph(SCO$_2$Me)$_2$)$^+$, 55%), and 105 (M – Ph$_2$SCO$_2$Me(CO$_2$Me))$^+$, 37%), as well as 60 ((COS)$^+$, 100%). Similarly was prepared Ph$_2$Ge[SCO$_2$(*i*-Pr)]$_2$, **17**, as a colorless solid (yield 81%). Peaks corresponding to ^{74}Ge were seen at *m/z* (relative intensity): 469 ((M)$^+$ 5%), 347 (M – SCO$_2$C$_3$H$_7$)$^+$, 32%), 287 (M – SCO$_2$C$_3$H$_7$(COS))$^+$, 82%), 229 (M – SCO$_2$C$_3$H$_7$(SCO$_2$C$_3$H$_6$))$^+$, 100%), and 183 (M – PhSCO$_2$C$_3$H$_7$(CO$_2$C$_3$H$_7$) $^+$, 3%). Recrystallization from a CH$_2$Cl$_2$–*n*-hexane mixture gave colorless crystals, mp 95–96°C, but they were not of X-ray quality. Similarly was formed Ph$_2$Ge[SCO$_2$(*n*-Pr)]$_2$, **18**, as a colorless oil (yield 81%). Peaks corresponding to ^{74}Ge were seen at *m/z* (relative intensity): 347 ((M–SCO$_2$C$_3$H$_7$)$^+$, 22%), 304 ((M–SCO$_2$C$_3$H$_7$(C$_3$H$_7$))$^+$, 6%), 287 ((M – SCO$_2$C$_3$H$_7$)(COS)]$^+$, 48%), 259 ((M – SCO$_2$C$_3$H$_7$(CO$_2$C$_3$H$_7$))$^+$, 10%), 229 ((M – SCO$_2$C$_3$H$_7$(SCO$_2$C$_3$H$_6$))$^+$, 54%), 183 ((M – PhSCO$_2$C$_3$H$_7$(CO$_2$C$_3$H$_7$)$^+$, 23%), and 151 ((M – Ph(SCO$_2$C$_3$H$_7$)$_2$)$^+$, 28%), along with 60 ((COS)+, 67%).

Synthesis of (*O*-organo monothiocarbonato)-trimethylgermanes

Me$_3$Ge[SCO$_2$Me], **19***, Me$_3$Ge[SCO$_2$(i-Pr)],* **20***, and Me$_3$Ge[SCO$_2$(*n*-Pr)],* **21**

Typically, Me$_3$GeCl (0.20 mL, 1.62 mmol) and CH$_2$Cl$_2$ (ca. 8 mL) were distilled onto NaSCO$_2$Me (0.22 g, 1.93 mmol) at –196°C. The mixture was stirred for 4 h at room temperature, followed by filtration and evaporation under vacuum to give Me$_3$Ge[SCO$_2$Me], **19**, as a colorless liquid (0.25 g, 1.20 mmol, yield 74%), bp 82–84°C. Similarly were formed Me$_3$Ge[SCO$_2$(*i*-Pr)], **20**, a colorless liquid, yield 76%, bp 92–94°C, and Me$_3$Ge[SCO$_2$(*n*-Pr)], **21**, a colorless liquid, yield 73%, bp 88–90°C.

Attempted preparation of halodiphenylgermanium monothiocarbonates

Attempts to isolate samples of Ph$_2$GeCl[SCO$_2$R] species were not successful. Reactions with 1:1 molar ratios of Ph$_2$GeCl$_2$ and NaSCO$_2$R always gave mixtures of the halo and bis compounds, as was confirmed from the ^{1}H NMR spectra.

Physical measurements

The infrared spectra were recorded on a Nicolet 5DX FT spectrometer as KBr pellets or oils smeared between KBr windows in the region 4000–400 cm^{-1}, and far infrared spectra on a Bomem DA3 infrared spectrometer between polyethylene films as oils or Nujol mulls. The Raman spectra were recorded on samples in sealed glass capillaries on a JEOL-XY Raman spectrometer using the 5145 Å exciting line of an argon ion laser. The ^{1}H and ^{13}C {H}NMR spectra were recorded on a Bruker 300 FT/NMR spectrometer at 300.133 and 75.471 MHz, respectively, in CDCl$_3$ using Me$_4$Si as internal standard. All NMR spectra were run at ambient temperature, with the exception of the routine VT NMR studies, and under standard operating conditions. The melting points were determined on a Fisher–Johns apparatus. The mass spectra were recorded on a Kratos Profile GC–MS spectrometer.

X-ray crystallographic analysis

Crystals of Me$_2$Ge[S$_2$CSEt]$_2$, **1**, were grown from carbon disulfide at –15°C and those of Ph$_3$Ge[SCO$_2$Me], **13**, Ph$_3$Ge[SCO$_2$(*i*-Pr)], **14**, and Ph$_2$Ge[SCO$_2$Me]$_2$, **16**, from CH$_2$Cl$_2$–*n*-hexane mixtures at 5°C. A yellow block crystal of **1** and colorless block crystals of **13, 14**, and **16**, of approximate dimensions 0.38 × 0.24 × 0.18, 0.30 × 0.30 × 0.21, 0.34 × 0.25 × 0.20, and 0.35 × 0.26 × 0.23 mm, respectively, were sealed in thin-walled glass capillaries and mounted on a Rigaku AFC6S diffractometer, with graphite-monochromated Mo Kα radiation.

Data collection was carried out as reported in detail earlier (10) and the important parameters are included in Table 1. Of the 1672 (**1**), 3597 (**13**), 7522 (**14**), and 3645 (**16**) reflections that were collected, 1536 (**1**), 3386 (**13**), 7178 (**14**), and 3645 (**16**) were unique. The intensities of three representative reflections measured after every 150 reflections remained constant throughout data collection, indicating crystal and electronic stability (no decay correction was applied for **1**, **13**, and **16**). However, over the course of data collection the standards decreased by 8.2% for **14**, so a linear correction factor was applied. The linear absorption coefficient for Mo Kα is 26.6 for **1**, 16.8 for **13**, 15.8 for **14**, and 18.7 cm^{-1} for **16**. An empirical absorption correction, based on azimuthal scans of several reflections, was applied that resulted in transmission factors ranging from 0.59 to 1.00 for **1**, 0.81 to 1.00 for **13**, 0.78 to 1.00 for **14**, and 0.77 to 1.00 for **16**. The data were corrected for Lorentz and polarization effects.

The structure was solved by direct methods (24) and all

Table 1. Summary of crystal data, intensity collection, and structural refinement for $Me_2Ge[S_2CSEt]_2$, **1**, $Ph_3Ge[SCO_2Me]$, **13**, $Ph_3Ge[SCO_2(i\text{-}Pr)]$, **14**, and $Ph_2Ge[SCO_2Me]_2$, **16**.

Parameter	1	13	14	16
Cell constants				
a (Å)	6.647(4)	9.970(4)	14.386(7)	11.790(4)
b (Å)	7.423(2)	10.660(3)	18.598(6)	13.696(5)
c (Å)	16.290(4)	9.853(2)	9.223(3)	23.232(6)
α (deg)	90.00	101.78(2)	102.85(3)	90.00
β (deg)	91.07(3)	109.98(2)	94.58(3)	92.26(3)
γ (deg)	90.00	89.76(3)	108.13(3)	90.00
Cell volume (Å^3)	803.6(4)	961.0(5)	2256(1)	3748(2)
Crystal system	monoclinic	triclinic	triclinic	monoclinic
Space group	$P2_1/m$	$P\bar{1}$	$P\bar{1}$	Cc
Mol.wt (g mol^{-1})	377.16	395.01	477.00	409.01
Z	2	2	2	8
Temperature (°C)	–30	23	23	23
ρ_{calcd} (g cm^{-3})	1.56	1.37	1.369	1.45
Absorption coefficient μ (cm^{-1})	26.55	16.8	15.82	18.70
Transmission factors	0.59–1.00	0.81–1.00	0.78–1.00	0.84–1.07
Radiation	MoKα 0.71609 Å			
Monochromater	Highly oriented graphite			
Max 2θ angle	50	50	50	50
Total reflections measured	1672	3597	7522	3645
Unique data used	771	1440	1725	1944
No. of parameters refined (NP)	88	127	214	225
$R = \Sigma\|\|F_o\| - \|F_c\|\|/\Sigma\|F_o\|$	0.0484	0.0534	0.0545	0.0563
$R_w = [(\Sigma w(\|F_o\| - \|F_c\|)^2/ \Sigma wF_o^2)]$	0.0485	0.0451	0.0552	0.0512
Goodness of fit	1.88	1.63	1.50	2.06
Largest shift/esd, final cycle	0.001	0.001	0.001	0.001
Largest resid elect density (e Å^{-3})	0.76	0.43	0.57	0.63

calculations were performed using the TEXSAN (25) crystallographic software package of Molecular Structure Corp. The non-hydrogen atoms were refined anisotropically and the hydrogen atoms were included in their idealized position with C—H set at 0.95 Å and with isotropic thermal parameters set at 1.2 times that of the carbon atom to which they were attached. The final cycle of full-matrix least-squares refinement[3] was based on 771 (**1**), 1440 (**13**), 1725 (**14**), and 1944 (**16**) observed reflections ($I\ 3.00\sigma(I)$) and 88 (**1**), 127 (**13**), 214 (**14**), and 225 (**16**) variable parameters and converged (largest parameter shift was 0.001 times its esd) with unweighted and weighted agreement factors of $R = \Sigma\,|\,|F_o| - |F_c|\,|\,/\,|F_c| =$ 0.0485 (**1**), 0.0534 (**13**), 0.0545 (**14**), and 0.0563 (**16**) and $R_w = [(\Sigma w(|F_o| - |F_c|)^2 / F_o^2)]^{1/2} =$ 0.0485 (**1**), 0.0451 (**13**), 0.0552 (**14**), and 0.0512 (**16**). The standard deviation of an observation of unit weight[4] was 1.88 (**1**), 1.63 (**13**), 1.50 (**14**), and 2.06 (**16**). The refinement of **16** was carried out on both enantiomorphs by inverting the structure and the better solution chosen. The maximum and minimum peaks on the final difference Fourier map corresponded to 0.86 and –0.62 e/Å^3, respectively, for **1**; 0.43 and –0.38 e/Å^3, respectively, for **13**; 0.57 and –0.40 e/Å^3, respectively, for **14**; and 0.63 and –0.53 e/Å^3, respectively, for **16**.

Table 2. Final fractional coordinates and B(eq) for non-hydrogen atoms of $Me_2Ge[S_2CSEt]_2$, **1**, with standard deviations in parentheses.

Atom	x	y	z	B(eq)
Ge(1)	0.0127(2)	1/4	0.7452(1)	3.56(7)
S(1)	–0.3109(5)	1/4	0.7920(2)	4.1(2)
S(2)	–0.0433(6)	1/4	0.9427(3)	5.4(2)
S(3)	–0.4925(5)	1/4	0.9481(2)	3.7(2)
S(4)	–0.1083(5)	1/4	0.6123(2)	4.2(2)
S(5)	0.3389(6)	1/4	0.6158(3)	7.8(3)
S(6)	0.0951(6)	1/4	0.4599(3)	5.4(2)
C(1)	–0.266(2)	1/4	0.8998(8)	3.2(6)
C(2)	–0.421(2)	1/4	1.0565(8)	4.1(8)
C(3)	–0.607(3)	1/4	1.104(1)	6(1)
C(4)	0.124(2)	1/4	0.566(1)	5.0(9)
C(5)	0.354(3)	1/4	0.427(1)	8(1)
C(6)	0.366(3)	1/4	0.340(1)	9(1)
C(7)	0.131(1)	0.018(2)	0.7705(6)	5.2(6)

The final atomic coordinates and equivalent isotropic thermal parameters for the non-hydrogen atoms are given in Tables 2–5, important distances and bond angles in Tables 6–9, and ORTEP diagrams in Figs. 1–4. Tables of final anisotropic

---

[3] Least-squares function minimized: $\Sigma w(|F_o| - |F_c|)^2$, where $w = 4F_o^2(F_o^2)$, $\sigma^2(F_o^2) = [S^2(C + R^2B) + pF_o^2)^2]/(\mathrm{Lp})^2$, S = scan rate, C = total integrated peak count, R = ratio of scan time to background counting time, Lp = Lorentz-polarization factor, and $p = p$ factor.

[4] Standard deviation of an observation of unit weight: $[\Sigma w(|F_o| - |F_c|)^2/N_o - N_v)^{1/2}]$, where N_o = number of observations and N_v = number of variables.

Table 3. Final fractional coordinates and *B*(eq) for non-hydrogen atoms of $Ph_3Ge[SCO_2Me]$, **13**, with standard deviations in parentheses.

Atom	*x*	*y*	*z*	*B*(eq)
Ge(1)	0.8021(1)	0.1505(1)	0.1526(1)	3.68(4)
S(1)	0.6413(3)	0.2207(2)	0.2601(3)	4.9(1)
O(1)	0.6728(8)	0.4161(6)	0.1430(8)	5.4(3)
O(2)	0.5102(7)	0.4219(6)	0.2543(7)	5.2(3)
C(1)	0.612(1)	0.370(1)	0.208(1)	4.1(5)
C(2)	0.469(1)	0.544(1)	0.217(1)	7.2(6)
C(3)	0.730(1)	0.1554(8)	–0.055(1)	3.7(2)
C(4)	0.588(1)	0.1192(9)	–0.143(1)	4.6(2)
C(5)	0.541(1)	0.114(1)	–0.294(1)	5.4(2)
C(6)	0.634(1)	0.147(1)	–0.357(1)	5.2(2)
C(7)	0.773(1)	0.186(1)	–0.272(1)	5.7(3)
C(8)	0.825(1)	0.191(1)	–0.119(1)	4.9(2)
C(9)	0.991(1)	0.2392(9)	0.257(1)	3.9(2)
C(10)	1.009(1)	0.370(1)	0.317(1)	7.8(3)
C(11)	1.151(1)	0.430(1)	0.387(1)	8.3(4)
C(12)	1.261(1)	0.360(1)	0.393(1)	7.0(3)
C(13)	1.248(1)	0.234(1)	0.344(1)	6.9(3)
C(14)	1.107(1)	0.172(1)	0.270(1)	5.6(3)
C(15)	0.809(1)	–0.0272(9)	0.176(1)	4.0(2)
C(16)	0.773(1)	–0.127(1)	0.052(1)	5.1(2)
C(17)	0.781(1)	–0.254(1)	0.071(1)	6.2(3)
C(18)	0.822(1)	–0.277(1)	0.208(1)	6.6(3)
C(19)	0.856(1)	–0.182(1)	0.331(1)	6.5(3)
C(20)	0.851(1)	–0.054(1)	0.317(1)	5.3(2)

Table 4. Final fractional coordinates and *B*(eq) for non-hydrogen atoms of $Ph_3Ge[SCO_2(i\text{-Pr})]$, **14**, with standard deviations in parentheses.

Atom	*x*	*y*	*z*	*B*(eq)
Ge(1)	0.9640(2)	0.8101(1)	0.4295(2)	3.4(1)
Ge(2)	0.4446(1)	0.3182(1)	–0.0880(2)	3.1(1)
Cl(1)	0.6910(6)	0.1257(5)	0.9721(9)	12.2(4)
Cl(2)	0.6209(7)	0.0436(5)	0.665(1)	13.4(5)
S(1)	1.1066(4)	0.8712(3)	0.5929(6)	4.7(3)
S(2)	0.5905(4)	0.3769(3)	0.0696(6)	8(2)
O(1)	1.159(1)	0.7761(9)	0.381(1)	5.7(7)
O(2)	1.258(1)	0.8311(8)	0.605(2)	5.9(7)
O(3)	0.643(1)	0.2956(8)	–0.167(1)	4.7(6)
O(4)	0.761(1)	0.3719(7)	0.032(1)	4.9(6)
C(1)	1.183(1)	0.821(1)	0.508(2)	4(1)
C(2)	1.321(2)	0.784(1)	0.560(2)	6(1)
C(3)	1.281(2)	0.710(2)	0.605(3)	10(2)
C(4)	1.424(2)	0.835(1)	0.640(3)	9(1)
C(5)	0.9335(9)	0.6982(5)	0.395(2)	4.9
C(6)	0.9620(8)	0.6679(7)	0.510(1)	4.9
C(7)	0.9354(9)	0.5870(8)	0.488(1)	4.9
C(8)	0.8803(9)	0.5364(5)	0.352(2)	4.9
C(9)	0.8518(8)	0.5667(7)	0.237(1)	4.9
C(10)	0.8784(9)	0.6476(8)	0.259(1)	4.9
C(11)	0.966(1)	0.8428(7)	0.243(1)	4.8
C(12)	1.0299(8)	0.8267(6)	0.145(1)	4.8
C(13)	1.0312(8)	0.8510(7)	0.012(1)	4.8
C(14)	0.969(1)	0.8914(7)	–0.022(1)	4.8
C(15)	0.9051(8)	0.9075(6)	0.077(1)	4.8
C(16)	0.9037(8)	0.8831(7)	0.210(1)	4.8
C(17)	0.8750(9)	0.8476(8)	0.548(1)	4.6
C(18)	0.794(1)	0.7940(5)	0.584(1)	4.6
C(19)	0.7295(7)	0.8206(7)	0.669(1)	4.6
C(20)	0.7464(8)	0.9008(9)	0.719(1)	4.6
C(21)	0.828(1)	0.9544(5)	0.683(1)	4.6
C(22)	0.8919(7)	0.9278(7)	0.598(1)	4.6
C(23)	0.667(1)	0.338(1)	–0.048(2)	3.2(9)
C(24)	0.835(1)	0.352(1)	–0.049(2)	5(1)
C(25)	0.869(2)	0.404(1)	–0.147(3)	8(1)
C(26)	0.919(2)	0.357(1)	0.068(2)	7.3(6)
C(27)	0.4120(8)	0.2056(5)	–0.125(2)	4.7
C(28)	0.4304(8)	0.1705(7)	–0.012(1)	4.7
C(29)	0.4014(8)	0.0891(8)	–0.043(1)	4.7
C(30)	0.3542(9)	0.0427(5)	–0.187(1)	4.7
C(31)	0.3358(8)	0.0778(7)	–0.300(1)	4.7
C(32)	0.3647(8)	0.1593(8)	–0.269(1)	4.7
C(33)	0.3569(9)	0.3550(8)	0.034(1)	4.4
C(34)	0.272(1)	0.3017(5)	0.061(1)	4.4
C(35)	0.2061(7)	0.3286(7)	0.142(1)	4.4
C(36)	0.2252(8)	0.4090(8)	0.196(1)	4.4
C(37)	0.310(1)	0.4623(5)	0.169(1)	4.4
C(38)	0.3761(7)	0.4354(7)	0.088(1)	4.4
C(39)	0.444(1)	0.3539(7)	–0.270(1)	4.7
C(40)	0.4973(8)	0.3349(6)	–0.384(1)	4.7
C(41)	0.4895(8)	0.3599(7)	–0.515(1)	4.7
C(42)	0.428(1)	0.4039(7)	–0.532(1)	4.7
C(43)	0.3752(8)	0.4228(6)	–0.418(1)	4.7
C(44)	0.3831(8)	0.3978(7)	–0.287(1)	4.7
C(45)	0.634(2)	0.121(1)	0.800(3)	10(1)

thermal parameters of non-hydrogen atoms, and fractional coordinates and thermal parameters of hydrogen atoms have been deposited.[5]

Results and discussion

The synthesis of bis(*S*-alkyl trithiocarbonato)dimethylgermanes, **1**–**4**, chloro(*S*-alkyl trithiocarbonato)diphenylgermanes, **5**–**8**, (*O*-alkyl monothiocarbonato)triphenylgermanes, **13**–**15**, bis(*O*-alkyl monothiocarbonato)diphenylgermanes, **16**–**18**, and (*O*-alkyl monothiocarbonato)trimethylgermanes, **19**–**21**, can be readily achieved in 73–90% yield by the reaction of the salt of the appropriate thiocarbonic acid in dried CS_2, CH_3Cl, or CH_2Cl_2 as solvent, or monothiocarbonic acid in dried CH_2Cl_2 as solvent with chlorotriphenylgermane, dichlorodiphenylgermane, or chlorotrimethylgermane using a standard Schlenk line in accord with eqs. [1]–[5]:

$$[1]\quad Me_2GeCl_2 + 2KS_2CSR \rightarrow Me_2Ge[S_2CSR]_2 + 2KCl$$

$$[2]\quad Ph_2GeCl_2 + KS_2CSR \rightarrow Ph_2GeCl[S_2CSR] + KCl$$

(R = Et, *i*-Pr, *n*-Pr, *n*-Bu)

---

[5] Copies of material deposited may be purchased from: The Depository of Unpublished Data, Document Delivery, CISTI, National Research Council Canada, Ottawa, ON K1A 0S2, Canada. Tables of atomic coordinates have been deposited with the Cambridge Crystallographic Centre, and can be obtained on request from The Director, Cambridge Crystallographic Centre, University Chemical Laboratory, 12 Union Road, Cambridge CB2 1EZ, U.K. Structure factor amplitudes are no longer being deposited and may be obtained directly from the author.

Table 5. Final fractional coordinates and B(eq) for non-hydrogen atoms of $Ph_2Ge[SCO_2Me]_2$, **16** with standard deviations in parentheses.

Atom	*x*	*y*	*z*	*B*(eq)
Ge(1)	0.2414	0.7159(1)	0.3834	3.31(8)
Ge(2)	–0.0090(2)	0.9707(1)	0.08263(9)	3.38(9)
S(1)	0.2911(5)	0.8261(3)	0.4521(2)	4.9(3)
S(2)	0.2123(5)	0.5951(4)	0.4470(2)	5.0(3)
S(3)	0.0181(5)	0.8536(4)	0.0163(2)	5.2(3)
S(4)	–0.0514(5)	1.0846(4)	0.0145(2)	4.9(3)
O(1)	0.292(1)	0.925(1)	0.3547(6)	5.9(8)
O(2)	0.334(2)	1.0076(9)	0.4359(6)	6.3(8)
O(3)	0.160(1)	0.5159(8)	0.3450(6)	5.4(8)
O(4)	0.142(1)	0.4248(9)	0.4237(5)	5.5(7)
O(5)	0.052(1)	0.764(1)	0.1165(6)	5.8(8)
O(6)	0.090(1)	0.6841(9)	0.0344(6)	6.3(8)
O(7)	–0.050(1)	1.1861(9)	0.1118(7)	5.8(8)
O(8)	–0.103(2)	1.259(1)	0.0293(7)	8(1)
C(1)	0.304(2)	0.928(1)	0.405(1)	5(1)
C(2)	0.353(3)	1.096(2)	0.401(2)	12(2)
C(3)	0.168(2)	0.506(1)	0.396(1)	3.6(9)
C(4)	0.102(2)	0.342(2)	0.387(1)	9(2)
C(5)	0.368(1)	0.684(1)	0.3368(6)	5.9
C(6)	0.454(1)	0.615(1)	0.3490(5)	5.9
C(7)	0.543(1)	0.6047(9)	0.3119(6)	5.9
C(8)	0.547(1)	0.662(1)	0.2625(6)	5.9
C(9)	0.462(1)	0.731(1)	0.2503(5)	5.9
C(10)	0.372(1)	0.7414(9)	0.2874(6)	5.9
C(11)	0.1002(8)	0.753(1)	0.3443(5)	5.3
C(12)	0.024(1)	0.804(1)	0.3777(4)	5.3
C(13)	–0.080(1)	0.8335(8)	0.3536(5)	5.3
C(14)	–0.1091(8)	0.8121(9)	0.2962(5)	5.3
C(15)	–0.033(1)	0.761(1)	0.2628(4)	5.3
C(16)	0.071(1)	0.7312(8)	0.2869(5)	5.3
C(17)	0.056(2)	0.758(1)	0.065(1)	5(1)
C(18)	0.122(2)	0.598(1)	0.070(1)	7(1)
C(19)	–0.069(2)	1.184(1)	0.0609(9)	4(1)
C(20)	–0.126(3)	1.350(2)	0.061(1)	9(2)
C(21)	0.1297(9)	1.004(1)	0.1240(5)	5.3
C(22)	0.211(1)	1.0670(9)	0.1032(4)	5.3
C(23)	0.311(1)	1.0849(8)	0.1356(5)	5.3
C(24)	0.3297(9)	1.039(1)	0.1888(5)	5.3
C(25)	0.248(1)	0.976(1)	0.2096(4)	5.3
C(26)	0.148(1)	0.9578(8)	0.1772(5)	5.3
C(27)	–0.1376(8)	0.9442(9)	0.1294(5)	4.5
C(28)	–0.214(1)	0.8710(8)	0.1116(4)	4.5
C(29)	–0.3113(9)	0.8545(7)	0.1420(5)	4.5
C(30)	–0.3332(8)	0.9111(9)	0.1903(5)	4.5
C(31)	–0.257(1)	0.9842(8)	0.2081(4)	4.5
C(32)	–0.1595(9)	1.0007(8)	0.1776(5)	4.5

Table 6. Interatomic distances (Å) and angles (deg) for $Me_2Ge[S_2CSEt]_2$, **1**.

Ge(1)—S(1)	2.296(4)	Ge(1)—S(4)	2.294(4)
Ge(1)—C(7)	1.93(1)		
S(1)—C(1)	1.78(1)	S(4)—C(4)	1.73(1)
S(2)—C(1)	1.62(1)	S(5)—C(4)	1.63(2)
S(3)—C(1)	1.71(1)	S(6)—C(4)	1.74(2)
S(3)—C(2)	1.82(1)	S(6)—C(5)	1.81(2)
C(2)—C(3)	1.48(2)	C(5)—C(6)	1.43(2)
Ge(1)—S(2)	3.246(5)	Ge(1)—S(5)	3.051(5)
Ge(1)—S(3)	4.756(4)	Ge(1)—S(6)	4.688(1)
S(1)-Ge(1)-S(4)	90.0(1)	C(7)-Ge(1)-C(7)[a]	125.8(6)
S(1)-Ge(1)-C(7)	107.9(3)	S(1)-Ge(1)-C(7)[a]	107.9(3)
S(4)-Ge(1)-C(7)	109.6(3)	S(4)-Ge(1)-C(7)[a]	109.6(3)
Ge(1)-S(1)-C(1)	100.8(4)	Ge(1)-S(4)-C(4)	96.3(6)
S(1)-C(1)-S(2)	124.1(8)	S(4)-C(4)-S(5)	125(1)
S(1)-C(1)-S(3)	108.7(7)	S(4)-C(4)-S(6)	110.5(9)
S(2)-C(1)-S(3)	127.2(9)	S(5)-C(4)-S(6)	125.0(9)
C(1)-S(3)-C(2)	103.2(7)	C(4)-S(6)-C(5)	101.7(8)
S(3)-C(2)-C(3)	108(1)	S(6)-C(5)-C(6)	111(2)
S(1)-Ge(1)—S(2)	62.9(1)	S(4)-Ge(1)—S(5)	65.8(1)

[a] *x*, 1/2 – *y*, *z*.

Table 7. Interatomic distances (Å) and angles (deg) for $Ph_3Ge[SCO_2Me]$, **13**.

Ge(1)—S(1)	2.253(3)	Ge(1)—C(3)	1.931(9)
Ge(1)—C(9)	1.946(9)	Ge(1)—C(15)	1.950(9)
S(1)—C(1)	1.77(1)	O(1)—C(1)	1.19(1)
O(2)—C(1)	1.32(1)	O(2)—C(2)	1.45(1)
Ge(1)—O(1)	3.112(7)	Ge(1)—O(2)	4.331(7)
S(1)-Ge(1)-C(3)	110.6(3)	S(1)-Ge(1)-C(9)	112.8(3)
S(1)-Ge(1)-C(15)	100.4(3)	C(3)-Ge(1)-C(15)	110.1(4)
C(3)-Ge(1)-C(9)	112.8(4)	C(9)-Ge(1)-C(15)	109.4(4)
Ge(1)-S(1)-C(1)	99.6(4)	C(1)-O(2)-C(2)	115.1(8)
S(1)-C(1)-O(1)	125.9(8)	S(1)-C(1)-O(2)	107.8(7)
Ge(1)-C(3)-C(4)	121.8(7)	Ge(1)-C(3)-C(8)	119.1(7)
Ge(1)-C(9)-C(10)	122.1(8)	Ge(1)-C(9)-C(14)	119.2(8)
Ge(1)-C(15)-C(16)	119.9(7)	Ge(1)-C(15)-C(20)	120.1(7)
O(1)-C(1)-O(2)	126.0(1)	S(1)-Ge(1)—O(1)	56.4(1)
O(1)—Ge(1)-C(3)	75.4(3)	O(1)—Ge(1)-C(9)	89.0(3)
O(1)—Ge(1)-C(15)	155.5(3)		

$$[3] \quad Ph_3GeCl + NaSCO_2R \rightarrow Ph_3Ge[SCO_2R] + NaCl$$

$$[4] \quad Ph_2GeCl_2 + 2NaSCO_2R \rightarrow Ph_2Ge[SCO_2R]_2 + 2NaCl$$

$$[5] \quad Me_3GeCl + NaSCO_2R \rightarrow Me_3Ge[SCO_2R] + NaCl \qquad (R = Me,\ i\text{-}Pr,\ n\text{-}Pr)$$

The salts are used in considerable excess relative to the stoichiometric requirements to ensure complete reaction in eqs. [1], [3], [4], and [5] and exact stoichiometric amounts in eq. [2] to favor the formation of the mixed chloro derivatives. It is essential that the trithiocarbonate salts be carefully repurified before use to avoid side reactions leading to polysulfides (23), but monothiocarbonate salts can be used as prepared provided pure dry alcohol was used in their preparation.

Chloro(*S*-alkyl trithiocarbonato)diphenylgermanes react readily in situ with bromotrimethylsilane in CS_2 or CH_2Cl_2 to give bromo(*S*-alkyl trithiocarbonato)diphenylgermanes, **9**–**12**, in accord with eq. [6]. An excess of Me_3SiBr is used as both it and Me_3SiCl are readily volatile and so are easily separated from the products.

$$[6] \quad Ph_2GeCl[S_2CSR] + Me_3SiBr \rightarrow Ph_2GeBr[S_2CSR] + Me_3SiCl \qquad (R = Et,\ i\text{-}Pr,\ n\text{-}Pr,\ n\text{-}Bu)$$

Table 8. Interatomic distances (Å) and angles (deg) for $Ph_3Ge[SCO_2(i\text{-}Pr)]$, **14**.

Ge(1)—S(1)	2.251(5)	Ge(2)—S(2)	2.256(5)
Ge(1)—C(5)	1.93(1)	Ge(2)—C(27)	1.940(9)
Ge(1)—C(11)	1.94(1)	Ge(2)—C(33)	1.94(1)
Ge(1)—C(17)	1.94(1)	Ge(2)—C(39)	1.94(1)
S(1)—C(1)	1.78(2)	S(2)—C(23)	1.80(2)
O(1)—C(1)	1.23(2)	O(3)—C(23)	1.16(2)
O(2)—C(1)	1.28(3)	O(4)—C(23)	1.38(2)
O(2)—C(2)	1.48(3)	O(4)—C(24)	1.44(3)
C(2)—C(3)	1.48(4)	C(24)—C(25)	1.47(4)
C(2)—C(4)	1.51(3)	C(24)—C(26)	1.51(3)
Ge(1)—O(1)	3.10(2)	Ge(2)—O(3)	3.13(2)
Ge(1)—O(2)	4.27(2)	Ge(2)—O(4)	4.34(1)
S(1)-Ge(1)-C(5)	108.4(4)	S(2)-Ge(2)-C(27)	108.3(4)
S(1)-Ge(1)-C(11)	113.2(4)	S(2)-Ge(2)-C(33)	100.8(3)
S(1)-Ge(1)-C(17)	99.4(3)	S(2)-Ge(2)-C(39)	112.7(4)
C(5)-Ge(1)-C(11)	112.5(5)	C(27)-Ge(2)-C(33)	111.4(6)
C(5)-Ge(1)-C(17)	112.1(5)	C(27)-Ge(2)-C(39)	113.7(5)
C(11)-Ge(1)-C(17)	110.5(6)	C(11)-Ge(2)-C(39)	109.3(6)
Ge(1)-S(1)-C(1)	100.5(6)	Ge(2)-S(2)-C(23)	98.3(6)
S(1)-C(1)-O(1)	123(2)	S(2)-C(23)-O(3)	128(2)
S(1)-C(1)-O(2)	110(2)	S(2)-C(23)-O(4)	105(1)
O(1)-C(1)-O(2)	127(2)	O(3)-C(23)-O(4)	127(2)
C(1)-O(2)-C(2)	117(2)	C(23)-O(4)-C(24)	114(1)
O(2)-C(2)-C(3)	107(2)	O(4)-C(24)-C(25)	111(2)
O(2)-C(2)-C(4)	105(2)	O(4)-C(24)-C(26)	107(2)
C(3)-C(2)-C(4)	115(2)	C(25)-C(24)-C(26)	112(2)
Ge(1)-C(5)-C(6)	119.8(8)	Ge(2)-C(27)-C(28)	122.2(8)
Ge(1)-C(5)-C(10)	120(1)	Ge(2)-C(27)-C(32)	118(1)
Ge(1)-C(11)-C(12)	121(1)	Ge(2)-C(33)-C(34)	120(1)
Ge(1)-C(11)-C(16)	119.4(9)	Ge(2)-C(33)-C(38)	119.7(9)
Ge(1)-C(17)-C(18)	120(1)	Ge(2)-C(39)-C(40)	124(1)
Ge(1)-C(17)-C(22)	120.3(9)	Ge(2)-C(39)-C(44)	116.4(9)
S(1)-Ge(1)—O1()	56.7(3)	S(2)-Ge(2)—O3()	56.8(3)
O(1)—Ge(1)-C(5)	72.9(5)	O(2)—Ge(2)-C(27)	77.9(5)
O(1)—Ge(1)-C(11)	88.6(5)	O(2)—Ge(2)-C(33)	157.5(4)
O(1)—Ge(1)-C(17)	154.8(4)	O(2)—Ge(2)-C(39)	83.6(5)

Table 9. Interatomic distances (Å) and angles (deg) for $Ph_2Ge[SCO_2Me]_2$, **16**.

Ge(1)—S(1)	2.257(5)	Ge(2)—S(3)	2.255(6)
Ge(1)—S(2)	2.255(5)	Ge(2)—S(4)	2.264(5)
Ge(1)—C(5)	1.93(1)	Ge(2)—C(21)	1.92(1)
Ge(1)—C(11)	1.93(1)	Ge(2)—C(27)	1.93(1)
S(1)—C(1)	1.78(2)	S(3)—C(17)	1.77(2)
S(2)—C(3)	1.77(2)	S(4)—C(19)	1.76(2)
O(1)—C(1)	1.18(3)	O(5)—C(17)	1.20(3)
O(2)—C(1)	1.34(2)	O(6)—C(17)	1.31(3)
O(2)—C(2)	1.47(3)	O(6)—C(18)	1.49(3)
O(3)—C(3)	1.19(3)	O(7)—C(19)	1.20(3)
O(4)—C(3)	1.33(2)	O(8)—C(19)	1.32(2)
O(4)—C(4)	1.48(3)	O(8)—C(20)	1.47(3)
Ge(1)—O(1)	3.00(1)	Ge(2)—O(5)	3.02(1)
Ge(1)—O(2)	4.30(1)	Ge(2)—O(6)	4.26(1)
Ge(1)—O(3)	3.03(1)	Ge(2)—O(7)	3.07(1)
Ge(1)—O(4)	4.27(1)	Ge(2)—O(8)	4.28(2)
S(1)-Ge(1)-S(2)	93.9(2)	S(3)-Ge(2)-S(4)	92.6(2)
S(1)-Ge(1)-C(5)	111.4(4)	S(3)-Ge(2)-C(21)	111.6(4)
S(1)-Ge(1)-C(11)	110.7(4)	S(3)-Ge(2)-C(27)	112.7(4)
S(2)-Ge(1)-C(5)	109.9(5)	S(4)-Ge(2)-C(21)	110.5(4)
S(2)-Ge(1)-C(11)	110.4(4)	S(4)-Ge(2)-C(27)	111.5(4)
C(5)-Ge(1)-C(11)	117.9(5)	C(21)-Ge(2)-C(27)	115.7(5)
Ge(1)-S(1)-C(1)	96.8(7)	Ge(2)-S(3)-C(17)	97.3(7)
S(1)-C(1)-O(1)	124(1)	S(3)-C(17)-O(5)	125(2)
S(1)-C(1)-O(2)	110(2)	S(3)-C(17)-O(6)	107(2)
O(1)-C(1)-O(2)	126(2)	O(5)-C(17)-O(6)	128(2)
C(1)-O(2)-C(2)	115(2)	C(17)-O(6)-C(18)	113(2)
Ge(1)-S(2)-C(3)	96.5(7)	Ge(2)-S(4)-C(19)	97.8(7)
S(2)-C(3)-O(3)	127(1)	S(4)-C(19)-O(7)	127(1)
S(2)-C(3)-O(4)	109(1)	S(4)-C(19)-O(8)	108(1)
O(3)-C(3)-O(4)	124(2)	O(7)-C(19)-O(8)	125(2)
C(3)-O(4)-C(4)	116(2)	C(19)-O(8)-C(20)	116(2)
Ge(1)-C(5)-C(6)	127(1)	Ge(2)-C(21)-C(22)	123.8(9)
Ge(1)-C(5)-C(10)	112.5(9)	Ge(2)-C(21)-C(26)	116.2(8)
Ge(1)-C(11)-C(12)	115.4(9)	Ge(2)-C(27)-C(28)	118.5(8)
Ge(1)-C(11)-C(16)	124.6(9)	Ge(2)-C(27)-C(32)	121.4(8)
S(1)-Ge(1)—O(1)	58.1(1)	S(3)-Ge(2)—O(5)	58.1(3)
S(2)-Ge(1)—O(3)	58.3(1)	S(4)-Ge(2)—O(7)	57.3(3)
S(2)-Ge(1)—O(1)	151.9(3)	S(4)-Ge(2)—O(5)	150.7(3)
S(1)-Ge(1)—O(3)	152.1(3)	S(3)-Ge(2)—O(7)	149.6(3)
O(1)—Ge(1)—O(3)	149.4(4)	O(5)—Ge(2)—O(7)	152.0(4)

In general, all of the compounds are susceptible to moisture and air on exposure to the atmosphere, as was found for the corresponding dithiocarbonates as well as for the related trithiocarbonates reported earlier (15). This appears to be especially true for the bis-diphenyl derivatives, **16**–**18**, where the formation of crystals of $(Ph_2GeO)_3$, the ring trimer of diphenylgermanium oxide, was confirmed by X-ray crystallography (26) when solutions of $Ph_2Ge[SCO_2R]_2$ species in CH_2Cl_2 are evaporated over several days while exposed to moist air. In addition, the trithiocarbonates, **1**–**12**, characteristically readily undergo carbon disulfide elimination at room temperature in accord with eqs. [7]–[9], so that all of the compounds are stored at –15°C in sealed containers.

[7] $Ph_2GeX[S_2CSR] \rightarrow Ph_2GeX[SR] + CS_2$

[8] $Me_2Ge[S_2CSR]_2 \rightarrow Me_2Ge[S_2CSR][SR] + CS_2$

[9] $Me_2Ge[S_2CSR][SR] \rightarrow Me_2Ge[SR]_2 + CS_2$

All compounds were readily dissolved in chloroform, which was therefore used as the preferred solvent for recording NMR spectra.

Carbon disulfide elimination

In all cases, for **2**–**12**, attempts to distill the yellow oils under vacuum or to warm them to obtain their boiling points resulted in the rapid expulsion of CS_2. As found with the $Ph_3Ge[S_2CSR]$ species (15), the ^1H and ^{13}C NMR spectra of sealed samples of solutions of compounds **1**–**12** held at room temperature showed a steady decrease in intensity of the signals attributable to $Me_2Ge[S_2CSR]_2$, **1**–**4**, or $Ph_2XGe[S_2CSR]$, **5**–**12**, species. Typically, in the ^{13}C NMR spectra, a peak at 192.7 ppm, attributable to CS_2, soon appeared and steadily increased in intensity with time as the peak originally observed in the range 225.68–226.70 ppm for **1**–**4** and 217.35–224.86

Table 10. ^{1}H chemical shifts in the NMR spectra of compounds **1**–**4** as well as the decomposition products Me$_2$Ge[S$_2$CSR][SR], where R = Et, *i*-Pr, *n*-Pr, and *n*-Bu.[a–c]

Compounds	Ge-CH_3	S-CH_n	SC-C$H_n{}'$	SCC-C$H_3{}''$
Me$_2$Ge[S$_2$CSEt]$_2$, **1**	1.43 (s)	3.06 (4H, q, 7.4)	1.20 (6H, t, 7.4)	
Me$_2$Ge[S$_2$CS(*i*-Pr)]$_2$, **2**	1.43 (s)	3.68 (2H, sept, 6.9)	1.26 (12H, d, 6.9)	
Me$_2$Ge[S$_2$CS(*n*-Pr)]$_2$, **3**	1.42 (s)	3.04 (4H, t, 7.4)	1.58 (4H, m, 7.4, 7.3)	0.90 (6H, t, 7.3)
Me$_2$Ge[S$_2$CS(*n*-Bu)]$_2$, **4**[d]	1.42 (s)	3.08 (4H, t, 7.3)	1.54 (4H, m ,7.3, 7.3)	1.31 (4H, m, 7.3, 7.3)
Me$_2$Ge[S$_2$CSEt]*[SEt]*	1.11 (s)	3.20 (2H, q, 7.4) *2.65 (2H, q, 7.4)*	1.30 (3H, t, 7.4) *1.28 (3H, t, 7.4)*	
Me$_2$Ge[S$_2$CS(*i*-Pr)]*[S(*i-*Pr)]*	1.12 (s)	3.88 (1H, sept, 6.8) *3.27 (1H, sept, 6.6)*	1.36 (6H, d, 6.8) *1.37 (6H, d, 6.6)*	
Me$_2$Ge[S$_2$CS(*n*-Pr)]*[S(*n-*Pr)]*	1.10 (s)	3.18 (2H, t, 7.3) *2.59 (2H, t, 7.3)*	1.69 (2H, m) *1.61 (2H, m)*	0.98 (3H, t, 7.5) *0.96 (3H, t, 7.5)*
Me$_2$Ge[S$_2$CS(*n*-Bu)]*[S(*n-*Bu)]*[e]	1.08 (s)	3.18 (2H, t, 7.4) *2.58 (2H, t, 7.4)*	1.62 (2H, m) *1.59 (2H, m)*	1.39 (2H, m) *1.37 (2H, m)*

[a] The spectra were recorded in CDCl$_3$ and are reported in ppm from Me$_4$Si, using CHCl$_3$ as a second standard.

[b] Multiplicities (s = singlet, d = doublet, t = triplet, sept = septet, m = multiplet), and coupling constants in Hz are given in parentheses.

[c] Peaks attributable to [SR] groups are in italics.

[d] Peaks also assigned to SC$_3$-CH_3“ at 0.86 (6H, t, 7.3).

[e] Peaks also assigned to SC$_3$-CH_3“ are seen at 0.89 (3H, t, 7.0) and *0.97 (3H, t, 7.3)*.

Table 11. ^{13}C chemical shifts in the NMR spectra of compounds **1**–**4** as well as the decomposition products Me$_2$Ge[S$_2$CSR][SR] where R = Et, *i*-Pr, *n*-Pr, and *n*-Bu.[a]

Compounds	Ge-*C*	S-*C*	SC-*C*	SC$_2$-*C*	SC$_3$-*C*	S$_2$*C*S
Me$_2$Ge[S$_2$CSEt]$_2$, **1**	9.83	34.16	12.70			226.11
Me$_2$Ge[S$_2$CS(*i*-Pr)]$_2$, **2**	9.92	44.96	21.73			225.68
Me$_2$Ge[S$_2$CS(*n*-Pr)]$_2$, **3**	9.86	41.89	21.29	13.64		226.28
Me$_2$Ge[S$_2$CS(*n*-Bu)]$_2$, **4**	9.87	39.79	29.74	22.22	13.72	226.26
Me$_2$Ge[S$_2$CSEt]*[SEt]*	5.82	33.84 *(22.60)*	12.69 *(18.68)*			226.53
Me$_2$Ge[S$_2$CS(*i*-Pr)]*[S(*i-*Pr)]*	6.21	44.45 *(34.35)*	21.73 *(27.82)*			226.12
Me$_2$Ge[S$_2$CS(*n*-Pr)]*[S(*n-*Pr)]*	5.88	41.56 *(30.28*)	21.29 *(26.46*)	13.84 *(13.43)*		226.70
Me$_2$Ge[S$_2$CS(*n*-Bu)]*[S(*n-*Bu)]*	5.83	39.40 *(35.15)*	29.81 *(27.91)*	21.83 *(22.22)*	13.72 *(13.55)*	226.64

[a] The spectra are recorded in CDCl$_3$ and are reported in ppm from Me$_4$Si.

Table 12. ^{1}H chemical shifts in the NMR spectra of compounds **5**–**12**.[a–c]

Compounds	Ge-C$_6H_5$	S-CH_n	SC-C$H_n{}'$	SCC-C$H_3{}''$
Ph$_2$GeCl[S$_2$CSEt], **5**	7.88–7.85 (4H) 7.53–7.45 (6H)	3.13 (2H, q, 7.4)	1.28 (3H, t, 7.5)	
Ph$_2$GeCl[S$_2$CS(*i*-Pr)], **6**	7.86–7.83 (4H) 7.49–7.46 (6H)	3.71 (1H, sept, 6.9)	1.34 (6H, d, 6.9)	
Ph$_2$GeCl[S$_2$CS(*n*-Pr)], **7**	7.87–7.84 (4H) 7.50–7.45 (6H)	3.10 (2H, t, 7.3)	1.66 (2H, m, 7.3, 7.4)	0.95 (3H, t, 7.4)
Ph$_2$GeCl[S$_2$CS(*n*-Bu)], **8**	7.86–7.83 (4H) 7.52–7.47 (6H)	3.11 (2H, t, 7.4)	1.60 (2H, m, 7.4, 7.5)	1.35 (2H, m, 7.5, 7.3)
Ph$_2$GeBr[S$_2$CSEt], **9**	7.73–7.70 (4H) 7.51–7.47 (6H)	3.26 (2H, q, 7.4)	1.33 (3H, t, 7.4)	
Ph$_2$GeBr[S$_2$CS(*i*-Pr)], **10**	7.75–7.72 (4H) 7.51–7.49 (6H)	3.92 (1H, sept, 6.9)	1.39 (6H, d, 6.9)	
Ph$_2$GeBr[S$_2$CS(*n*-Pr)], **11**	7.72–7.69 (4H) 7.49–7.46 (6H)	3.21 (2H, t, 7.3)	1.70 (2H, m, 7.3, 7.3)	0.99 (3H, t, 7.3)
Ph$_2$GeBr[S$_2$CS(*n*-Bu)], **12**	7.73–7.71 (4H) 7.50–7.49 (6H)	3.25 (2H, t, 7.4)	1.67 (2H, m, 7.4, 7.5)	1.42 (2H, m, 7.5, 7.3)

[a] The spectra were recorded in CDCl$_3$ and are reported in ppm from Me$_4$Si, using CHCl$_3$ as a second standard.

[b] Number of protons, multiplicities (d = doublet, t = triplet, sept = septet, m = multiplet), and coupling constants in Hz are given in parentheses.

[c] Peaks also assigned to SC$_3$-CH_3“ at 0.87 (3H, t, 7.3) for **8** and at 0.93 (3H, t, 7.3) for **12**.

Table 13. ^{13}C chemical shifts in the NMR spectra of compounds, **5**–**12**.[a,b]

Compounds	Ge-*C*$_6$	S-*C*	SC-*C*	SC$_2$-*C*	S$_2$*C*S
Ph$_2$GeCl[S$_2$CSEt], **5**	135.60, 133.77, 131.17, 128.88	34.51	12.55		224.63
Ph$_2$GeCl[S$_2$CS(*i*-Pr)], **6**	135.71, 133.73, 131.08, 128.84	45.56	21.64		224.27
Ph$_2$GeCl[S$_2$CS(*n*-Pr)], **7**	135.60, 133.76, 131.14, 128.88	42.21	21.13	13.58	224.86
Ph$_2$GeCl[S$_2$CS(*n*-Bu)], **8**	135.59, 133.73, 131.11, 128.84	40.11	29.53	22.18	224.83
Ph$_2$GeBr[S$_2$CSEt], **9**	135.38, 132.79, 131.76, 129.04	33.90	12.74		217.64
Ph$_2$GeBr[S$_2$CS(*i*-Pr)], **10**	135.38, 132.79, 131.62, 129.10	45.02	21.7		217.35
Ph$_2$GeBr[S$_2$CS(*n*-Pr)], **11**	135.31, 132.75, 131.79, 129.04	41.53	21.3	13.5	217.92
Ph$_2$GeBr[S$_2$CS(*n*-Bu)], **12**	135.38, 132.79, 131.76, 129.04	39.46	29.77	22.16	217.81

[a] The spectra are recorded in CDCl$_3$ and are reported in ppm from Me$_4$Si.

[b] Peaks attributable to SC$_3$-*C* are seen at 13.63 for **8** and at 13.71 for **12**.

Table 14. ^{1}H chemical shifts in the NMR spectra of compounds **13**–**21**.[a,b]

Compounds	Ge-C_6H_5/CH_3	O-CH_n	OC-CH_n	OCC-CH_3
$Ph_3Ge[SCO_2Me]$, **13**	7.64–7.61 (6H) 7.44–7.40 (9H)	3.58 (3H, s)		
$Ph_3Ge[SCO_2(i\text{-Pr})]$, **14**	7.64–7.61 (6H) 7.41–7.36 (9H)	4.86 (1H, sept, 6.4)	0.96 (6H, d, 6.4)	
$Ph_3Ge[SCO_2(n\text{-Pr})]$, **15**	7.64–7.61 (6H) 7.43–7.39 (9H)	3.93 (2H, t, 6.8)	1.42 (2H, m)	0.73 (3H, t, 7.4)
$Ph_2Ge[SCO_2Me]_2$, **16**	7.79–7.76 (4H) 7.48–7.45 (6H)	3.59 (6H, s)		
$Ph_2Ge[SCO_2(i\text{-Pr})]_2$, **17**	7.79–7.76 (4H) 7.45–7.43 (6H)	4.85 (2H, sept, 6.2)	0.99 (12H, d, 6.2)	
$Ph_2Ge[SCO_2(n\text{-Pr})]_2$, **18**	7.79–7.76 (4H) 7.49–7.43 (6H)	3.94 (4H, t, 6.9)	1.45 (4H, m)	0.75 (6H, t, 7.4)
$Me_3Ge[SCO_2Me]$, **19**	0.57 (9H)	3.65 (3H, s)		
$Me_3Ge[SCO_2(i\text{-Pr})]$, **20**	0.54 (9H)	4.91 (1H, sept, 6.3)	1.17 (6H, d, 6.3)	
$Me_3Ge[SCO_2(n\text{-Pr})]$, **21**	0.59 (9H)	4.04 (2H, t, 6.6)	1.62 (2H, m)	0.89 (3H, t, 7.4)

[a] The spectra were recorded in $CDCl_3$ and are reported in ppm from Me_4Si, using $CHCl_3$ as a second standard.

[b] Number of protons, multiplicities (d = doublet, t = triplet, sept = septet, m = multiplet), and coupling constants in Hz are given in parentheses.

Table 15. ^{13}C chemical shifts in the NMR spectra of compounds **13**–**21**.[a]

Compounds	Ge-C_6H_5/CH_3	O-C	OC-C	OC_2-C	SCO_2
$Ph_3Ge[SCO_2Me]$, **13**	134.74, 134.51, 130.14, 128.63	54.39			169.32
$Ph_3Ge[SCO_2(i\text{-Pr})]$, **14**	134.83, 134.71, 130.04, 128.56	72.20	21.48		168.05
$Ph_3Ge[SCO_2(n\text{-Pr})]$, **15**	134.71, 134.65, 130.07, 128.59	69.51	21.88	10.18	168.80
$Ph_2Ge[SCO_2Me]_2$, **16**	134.30, 133.93, 130.92, 128.70	54.75			168.61
$Ph_2Ge[SCO_2(i\text{-Pr})]_2$, **17**	134.61, 133.90, 130.76, 128.70	72.97	21.48		167.28
$Ph_2Ge[SCO_2(n\text{-Pr})]_2$, **18**	134.31, 133.92, 130.82, 128.72	69.97	21.83	10.15	168.08
$Me_3Ge[SCO_2Me]$, **19**	2.06	53.89			170.80
$Me_3Ge[SCO_2(i\text{-Pr})]$, **20**	2.21	71.23	21.90		169.49
$Me_3Ge[SCO_2(n\text{-Pr})]$, **21**	2.13	68.90	22.09	10.38	170.35

[a] The spectra were recorded in $CDCl_3$ and reported in ppm from Me_4Si.

Table 16. Selected features and their assignments in the vibrational spectra of compounds **1**–**4.**[a,b]

$Me_2Ge[S_2CSEt]_2$, **1**		$Me_2Ge[S_2CS(i\text{-Pr})]_2$, **2**		$Me_2Ge[S_2CS(n\text{-Pr})]_2$, **3**		$Me_2Ge[S_2CS(n\text{-Bu})]_2$, **4**		
IR	[Raman]	IR	[Raman]	IR	[Raman]	IR	[Raman]	Assignment
1066 s	[1072 (100)]	1067 vs	[1069 (55)]	1077 s	[1078 (60)]	1083 vs	[1082 (50)]	$\nu(S_2CSC)_a$
1033 s	[1026 (67]	1040 vs	[1039 (100)]	1043 vs	[1043 (100)]	1045 vs	[1047 (100)]	$\nu(S_2CSC)_b$
858 vs sh	[n.o.]	880 vs sh	[n.o.]	860 s sh	[n.o.]	860 s	[n.o.]	$\nu(H_3CGe)$
826 s	[827 (50)]	808 vs	[811 (5)]	819 vs	[815 (15)]	811 vs	[802 (25)]	$\nu(S_2CSC)_c$
623 m	[621 (20)]	627 m	[626 (20)]	626 m	[626 (20)]	626 m	[624 (35)]	$\nu(Ge\text{-}C)_{asym}$
569 w	[577 (65)]	616 m	[578 (40)]	580 m	[578 (50)]	578 m	[577 (50)]	$\nu(Ge\text{-}C)_{sym}$
509 w	[512 (65)]	531 w	[530 (70)]	510 w	[511 (80)]	509 m	[512 (75)]	$\nu(S_2CSC)_d$
407 m sh	[407 (54)]	406 m sh	[405 (50)]	416 m	[415 (50)]	406 m	[405 (55)]	$\nu(Ge\text{-}S)_{asym}$
360 m	[365 (35)]	360 w	[364 (30)]	373 m	[365 (40)]	388 s	[384 (20)]	$\nu(Ge\text{-}S)_{sym}$
314 m	[319 (20)]	329 s	[324 (20)]	319 m	[321 (15)]	328 m	[324 (10)]	$\delta(S_2CSC)$
194 w	[190 (50)]	213 m	[195 (50)]	191 w	[191 (75)]	191 s	[189 (75)]	$\rho(S_2CSC)$

[a] Parentheses denote relative intensities in the Raman effect.

[b] s = strong, m = medium, w = weak, sh = shoulder, br = broad, and v = very.

ppm for **5**–**12**, attributable to the S_2CS carbon, decreased in intensity to eventually disappear. As with the $Ph_2Ge[S_2CSR]_2$ series, more complicated spectra were observed between the NMR spectra of the freshly prepared $Me_2Ge[S_2CSR]_2$ species, **1**–**4**, and the final spectra that contained only peaks attributable to CS_2 and $Me_2Ge[SR]_2$. The additional peaks were entirely consistent with the formation of the intermediate $Me_2Ge[S_2CSR][SR]$ compounds, whose relevant ^{1}H and ^{13}C NMR data are also presented in Tables 10 and 11, respectively. For the three derivatives that are oils, **2**–**4**, CS_2 elimination is complete after approximately 5 days. The halodiphenyl derivatives **5**–**12** decompose even more rapidly, the original signals attributable to $Ph_2GeX[S_2CSR]$ being totally lost in 1–2 days to be replaced by peaks attributable to the corresponding $Ph_2GeX[SR]$ compounds.

Nuclear magnetic resonance spectra

For $Me_2Ge[S_2CSR]_2$, **1**–**4**, the ^{1}H NMR chemical shifts (Table 10) of methyl attached to Ge are similar for all trithiocarbonate derivatives, being dependent on the number of groups attached to Ge rather than the alkyl group of the ligand. Thus, the chemical shifts of CH_3-Ge are at 1.42–1.43 ppm for **1**–**4** compared to 0.71–0.73 ppm for $Me_3Ge[S_2CSR]$ (15). The same phenomenon was noted for $Me_2Ge[S_2CNMe_2]_2$ and

$Me_3Ge[S_2CNMe_2]$, suggesting the group electronegativities of trithiocarbonates and dithiocarbamates are similar (6). In general, all alkyl group peaks of the ligands have the fine structure and relative intensities expected for first-order spectra, except of course for the central CH_2 groups in *n*-propyl and *n*-butyl. The phenyl signals in $Ph_2GeCl[S_2CSR]$, **5**–**8**, are very similar in appearance and position to those reported for $Ph_2Ge[S_2CSR]_2$ (15) while those of $Ph_2GeBr[S_2CSR]$, **9**–**12**, are similar to $Ph_3Ge[S_2CSR]$ derivatives (Table 12). The chemical shifts within the ligands of these halo derivatives have values that differ systematically from the bis-diphenyl compounds, the proton shifts being increasingly upfield in the order bis < Cl < Br. The similarity of all spectra suggests the trithiocarbonate groups are in identical environments in all compounds **1**–**12**.

In the ^{13}C NMR spectra (Tables 11 and 13) the chemical shifts of the alkyl groups in the ligand are relatively similar regardless of the nature (methyl or phenyl) or number of groups attached to germanium. Comparison with the corresponding S_2COR derivatives (12, 13) indicates similar values for chemical shifts of all alkyl carbon atoms except for those directly attached to the sulfur atom, the difference in shift being consistently ca. 35 ppm as illustrated by that of CH_2 in $Me_2Ge[S_2CSCH_2CH_3]_2$ (33.84) and $Me_2Ge[S_2COCH_2CH_3]_2$ (71.10 ppm) (12). In contrast, there is an upfield shift of ca. 14 ppm for the central trithiocarbonate carbon atom so that S_2CS has chemical shifts of 225.68–226.28 ppm for **1**–**4** (Table 11) compared to 207.04–212.12 ppm for S_2CO in related dithiocarbonates (12, 13). For **5**–**12** (Table 13), the chemical shifts in ligands are basically the same as in the corresponding bis compounds, while for the S_2CS carbon in $Ph_2GeCl[S_2CSR]$ the shift is downfield relative to $Ph_2Ge[S_2CSR]_2$ (15) by ca. 2 ppm, but is upfield by ca. 5 ppm for $Ph_2GeBr[S_2CSR]$. As noted for the ^1H NMR spectra, the consistencies in the ^{13}C NMR spectra point to similar trithiocarbonate environments in compounds **1**–**12**.

The ^1H and ^{13}C NMR spectral data for monothiocarbonate compounds **13**–**21** are presented in Tables 14 and 15, respectively. The ^1H NMR spectra recorded in $CDCl_3$ confirm that the products are over 98% pure relative to any hydrogen-containing impurities and integration ratios are as expected. The signals due to the phenyl groups in compounds **13**–**18** (two sets of peaks between 7.36 and 7.79 ppm) are very similar in appearance and position to those of the analogous dithiocarbonate and trithiocarbonate series (15) as well as other phenylgermanium derivatives containing Ge—S bonds, so once again the chemical shifts are dependent on the presence of the Ge—S link(s) rather than the nature of the thiocarbonate groups attached to sulfur (4–14). The monothiocarbonate ligands again give first-order spectra when expected, with chemical shifts comparable to those of the corresponding salts. The chemical shifts of hydrogen atoms on the carbon atom attached to oxygen (i.e., $OCH/OCH_2/OCH_3$) are similar for a given monothiocarbonate regardless of the number of phenyl groups attached to germanium, as was observed for the corresponding OCH_n groups in analogous dithiocarbonates and SCH_n groups in trithiocarbonates. The chemical shifts in the O-linked monothiocarbonates lie between those of the O-linked dithiocarbonates and the S-linked trithiocarbonates, suggesting that the electronegativity of the SCO_2 group lies between those of S_2CO and S_2CS. In $Me_3Ge[SCO_2R]$ species **19**–**21**, the CH_3-Ge chemical shifts hardly vary, the values being slightly less than those reported for $Me_3Ge[S_2CNMe_2]$ and the $Me_3Ge[S_2CSR]$ derivatives (15), which is consistent with the group electronegativity of monothiocarbonates being slightly larger than those of dithiocarbamates (6) and trithiocarbonates. The similarity of all of the spectra again indicates that the environments of the monothiocarbonate groups in solution are identical in **13**–**21**.

In the ^{13}C NMR spectra, the chemical shifts of monothiocarbonate alkyl groups are again similar regardless of the number or nature of groups attached to germanium. The chemical shifts for the carbon atom of the SCO_2 groups in **13**–**21** range from 167.28 to 170.80 ppm, compared to 207.04 to 212.12 ppm for a variety of S_2CO groups, and 221.36 to 226.41 ppm for the S_2CS groups in the analogous trithiocarbonates. The $(CH_3)_3Ge$ chemical shifts are similar for **19, 20**, and **21** and are close to those of the analogous dithiocarbonates (11, 12) and trithiocarbonates. The general similarity of the values of the ^{13}C NMR chemical shifts in **13**–**21** is again consistent with the presence of similar monothiocarbonate linkages in solution.

Infrared and Raman spectra

Distinctive features in the infrared and Raman spectra and their assignments are given in Table 16 for $Me_2Ge[S_2CSR]_2$, **1**–**4**, and in Table 17 for $Ph_2GeCl[S_2CSR]$, **5**–**8**, and $Ph_2GeBr[S_2CSR]$, **9**–**12**. The assignments in the tables make use of such factors as the distinctive strong methyl germanium rocking mode at approximately 850 cm^{-1} (11); the pairs of fingerprints of decreasing intensity at ca. 740 and 695 cm^{-1}, 460 and 335 cm^{-1}, and 1435 and 1095 cm^{-1} in the infrared spectra for phenyl germanes and the very intense Raman peak close to 1000 cm^{-1} (12); comparisons with the spectra of previously reported related organogermanium trithiocarbonates; comparisons with the spectra of the starting salts, KS_2CSR; and the decrease in intensity of strong bands in the spectra of all of the compounds **1**–**24** as CS_2 elimination occurs. The labelling of the phenyl modes uses the Wiffen convention (27).

Typical values for C=S and C–S stretching vibrations are 1090 and 700 cm^{-1}, respectively, so assigning four specific stretches as $\nu(S{=}CS_2)$, $\nu(S_2C{-}SR)$, $\nu(S_2CS{-}C)$, and $\nu(GeS{-}CS_2)$ is not reasonable because the average positions of $\nu(S_2CSC)_a$, $\nu(S_2CSC)_b$, $\nu(S_2CSC)_c$, and $\nu(S_2CSC)_d$ are 1069, 1044, 826, and 515 cm^{-1}, respectively. Their similarity in all derivatives suggests that all are strongly coupled in a similar fashion and all have structures similar to those of $Me_2Ge[S_2CSEt]_2$, **1**, and $Ph_2Ge[S_2CS(i\text{-}Pr)]_2$ (15). The assignment of $\nu(S_2CSC)_d$ at ca. 515 cm^{-1} is close to that of the symmetric stretch in CS_3^{2-} (28), while the asymmetric stretch in CS_3^{2-} is typically seen in the range of 900–950 cm^{-1}, which is bracketed by the positions of $\nu(S_2CSC)_b$, and $\nu(S_2CSC)_c$. The asymmetric and symmetric Ge–C stretches are seen at ca. 626 and 580 cm^{-1} in all $Me_2Ge[S_2CSR]_2$, **1**–**4**, these values being similar to those in Me_2GeCl_2. The similarity of the position and separation between the modes indicates that **1**–**4** should have C-Ge-C angles as wide as that of 121(4)° in Me_2GeCl_2 (29). Table 6 confirms that the C-Ge-C angle in $Me_2Ge[S_2CSEt]_2$ is 128.8(6)°.

The Ge–Cl stretching vibration, ν(Ge–Cl), is close to 282 cm^{-1} in all $Ph_2GeCl[S_2CSR]$, **5**–**8**, compared to an average of ca. 400 cm^{-1} in Ph_2GeCl_2. A similar shift was noted for

Table 17. Selected features and their assignments in the vibrational spectra of compounds $Ph_2GeCl[S_2CSR]$ **5**–**8** and $Ph_2GeBr[S_2CSR]$, **9**–**12**, where R = Et, *i*-Pr, *n*-Pr, and *n*-Bu.[a–d]

5		**6**		**7**		**8**		**9**		**10**		**11**		**12**		
IR	[Raman]	IR	[Raman]	IR	[Raman]	IR	[Raman]	IR	[Raman]	IR	[Raman]	IR	[Raman]	IR	[Raman]	Assignment
1581 w	[1585 (25)]	1583 w	[1584 (25)]	1583 w	[1583 (30)]	1583 w	[n.o.]	1583 w	[1583 (30)]	1585 w	[1583 (35)]	15803 w	[1586 (30)]	1583 w	[1584 (20)]	*l*-Phenyl
1432 m		1433 vs		1433 m		1434 s		1434 s		1434 vs		1434 m		1434 s		*n*-Phenyl[d]
1186 w	[1187 (5)]	1184 ms	[n.o.]	1183 m	[1184 (10)]	1183 w	[n.o.]	1184 w	[1187 (5)]	1184 mw	[1187 (5)]	1184 w	[1185 (5)]	1183 w	[1184 (5)]	*a*-Phenyl
1158 w	[1158 (5)]	1157 s	[n.o.]	1159 w	[1155 (5)]	1158 vw	[1159 (5)]	1158 m	[1158 (5)]	1158 m	[1158 (5)]	1154 vw	[1150 (5)]	1160 w	[1161 (5)]	*e*-Phenyl
1088 s sh	[1085 (5)]	1091 vs	[1082 (5)]	1091 s	[1084 (5)]	1090 m	[1086 (10)]	1091 s	[1085 (10)]	1092 s	[1085 (5)]	1091 s	[1084 (5)]	1090 m	[1087 (10)]	*q*-Phenyl[c]
1072 vs	[n.o.]	1070 vs	[1070 (25)]	1058 s	[1070 (10)]	1066 s sh	[1070 (15)]	1067 m	[1063 (5)]	1068 m	[n.o.]	1063 m	[n.o.]	1060 m	[1060 (5)]	$\nu(S_2CSC)_a$
1044 s sh	[n.o.]	1039 vs	[1041 (35)]	1043 s	[1044 (10)]	1048 m	[1048 (25)]	1050 m	[n.o.]	1051 s	[n.o.]	1035 m	[n.o.]	1049 m	[1045 (15)]	$\nu(S_2CSC)_b$
1031 s	[1025 (10)]	1027 vs	[1026 (20)]	1026 s	[1025 (20)]	1026 m	[1026 (20)]	1025 m	[1025 (10)]	1026 m	[1025 (10)]	1025 s	[1027 (15)]	1026 m	[1026 (20)]	*b*-Phenyl
1004 m	[998 (100)]	998 s	[999 (100)]	998 m	[998 (100)]	998 m	[999 (100)]	998 s	[998 (100)]	998 s	[998 (100)]	998 m	[999 (100)]	998 m	[998 (100)]	*p*-Phenyl[c]
849 s		845 vs		840 s br		843 s br		820 s		821 s		819 m		819 m		$\nu(S_2CSC)_c$[d]
737 vs		736 vs		735 vs		735 vs		734 s		734 s		735 s		734 s		*f*-Phenyl[d]
692 s		692 vs		693 vs		692 vs		691 s		692 s		691 s		691 s		*v*-Phenyl[d]
675 s sh	[671 (10)]	669 mw	[668 (60)]	679 s sh	[669 (20)]	680 sh	[670 (30)]	674 m	[671 (15)]	674 m	[671 (15)]	674 w	[673 (15)]	676 m	[671 (10)]	*r*-Phenyl[c]
509 w	[517 (5)]	532 w	[532 (25)]	512 w	[512 (15)]	511 w	[512 (25)]	n.o.	[517 (5)]	524 w	[n.o.]	509 w	[n.o.]	508 w	[501 (25)]	$\nu(S_2CSC)_d$
459 s		459 vs		458 w		458 w		457 s		457 s		457 s		457 s		*y*-Phenyl[c,d]
411 s	[n.o.]	414 m	[429 (15)]	427 m	[428 (8)]	414 m	[420 (5)]	400 w	[n.o.]	403 w	[n.o.]	405 w	[n.o.]	401 m	[408 (5)]	ν(Ge-S)
365 m	[365 (45)]	363 s	[365 (50)]	367 m	[377 (60)]	366 m	[361 (10)]	318 m	[n.o]	315 s	[n.o.]	319 m	[n.o.]	320 s	[n.o.]	$\delta(S_2CSC)$
332 m		335 s		335 m		336 m		318 m		315 s		319 m		320 s		*t*-Phenyl[c,d]
283 s	[282 (10)]	282 m	[282 (10)]	284 s	[286 (50)]	280 m	[n.o.]	225 w	[224 (90)]	225 w[	224 (95)]	226 w	[223 (85)]	226 w	[225 (80)]	ν(Ge-X)
200 w	[196 (35)]	200 w	[196 (40)]	200 w	[204 (80)]	200 m	[200 (5)]	190 m	[193 (35)]	191 w	[193 (20)]	191 w	[198 (5]	195 m	[198 (5)]	$\rho(S_2CSC)$

[a] Parentheses denote relative intensities in the Raman effect.

[b] s = strong, m = medium, w = weak, sh = shoulder, br = broad, and v = very.

[c] X-sensitive modes.

[d] No corresponding modes observed in the Raman effect.

Table 18. Selected features and their assignments in the vibrational spectra of **13**–**15**.[a,b]

Ph$_3$Ge[SCO$_2$Me], **13**		Ph$_3$Ge[SCO$_2$(*i*-Pr)], **14**		Ph$_3$Ge[SCO$_2$(*n*-Pr)], **15**		
IR	Raman	IR	Raman	IR	Raman	Assignment
1695 vs	n.o.[c]	1695 vs	1700 (2)	1698 s	1696 (5)	$\nu(SCO_2C)_a$
n.o.	1585 (30)	n.o.	1587(20)	n.o.	1587 (30)	*l*-Phenyl
1428 s	1429 (1)	1428 s	n.o.	1435 ms	1435 (1)	*n*-Phenyl
1188 s	1188 (7)	1187 ms	n.o.	1185 m,sh	1184 (10)	*a*-Phenyl
1158 s,sh	1158 (7)	1162 s	n.o.	1164 m,sh	1158 (12)	*e*-Phenyl
1140 s	n.o.	1148 s	n.o.	1118 s	n.o.	$\nu(SCO_2C)_b$
1089 s	n.o.	1089 s	n.o.	1090 s	1089 (3)	$\nu(SC_2OC)_c$
1023 m	1027 (8)	1023 m	1025(10)	1027 s	1026 (20)	*b*-Phenyl
996 m	999 (100)	998 m	1001(100)	999 m	1001 (100)	*p*-Phenyl
815 ms	835 (2)	848 s	849 (1)	830 ms	840 (1)	$\pi(SCO_2)$
736 s	n.o.	737 s	n.o.	738 s	n.o.	*f*-Phenyl
697 s	n.o.	697 s	n.o.	699 s	n.o.	*v*-Phenyl
675 m,sh	668 (8)	675 m,sh	667 (10)	675 m	668 (15)	$\nu(SCO_2C)_d$ + *r*-phenyl
462 s	n.o.	468 s	n.o.	463 s,br	n.o.	*y*-Phenyl
419 m	428 (5)	436 m	430 (2)	424 m	n.o.	ν(Ge-S)

[a] Parentheses denote relative intensities in the Raman effect.
[b] s = strong, m = medium, sh = shoulder, br = broad.
[c] Not observed.

Table 19. Selected features and their assignments in the vibrational spectra of **16**–**18**.[a,b]

Ph$_2$Ge[SCO$_2$Me]$_2$, **16**		Ph$_2$Ge[SCO$_2$(*i*-Pr)]$_2$, **17**		Ph$_2$Ge[SCO$_2$(*n*-Pr)]$_2$, **18**		
IR	Raman	IR	Raman	IR	Raman	Assignment
1695 s	n.o.[c]	1698 s	1692 (8)	1702 s	1700 (2)	$\nu(SCO_2C)_a$
n.o.	1584 (40)	n.o.	1585 (30)	n.o.[c]	1578 (30)	*l*-Phenyl
1427 s	n.o.	1436 m	n.o.	1434 s	11432 (5)	*n*-Phenyl
1191 s	1187 (5)	1170 s,sh	1170 (5)	1170 s	n.o.	*a*-Phenyl
1134 s	n.o.	1159 s	n.o.	1132 vs	1156 (5)	$\nu(SCO_2C)_b$
1090 s	n.o.	1087 s	1090 (5)	1095 s	1080 (4)	$\nu(SCO_2C)_c$
1025 s	1027 (15)	1025 ms	1027 (20)	1023 s,sh	1026 (20)	*b*-Phenyl
998 m	999 (100)	999 m	1000 (100)	1000 m,sh	996 (100)	*p*-Phenyl
817 s	843 (30)	843 ms	846 (15)	833 m	843 (4)	$\pi(SCO_2)$
736 s	n.o.	738 m	n.o.	737 s	n.o.	*f*-Phenyl
693 s	n.o.	695 m,sh	n.o.	695 s	n.o.	*v*-Phenyl
678 s,br	678 (3)	673 m br	672 (2)	675 s	670 (10)	$\nu(SCO_2C)_d$ + *r*-phenyl
460 s	n.o.	461 m	n.o.	460 s	n.o.	*y*-Phenyl
434 ms	432 (2)	440 s	438 (15)	427 m	427 (3)	$\nu(Ge\text{-}S)_{asym}$
392 m	395 (1)	394 m	n.o.	390 s	392 (2)	$\nu(Ge\text{-}S)_{sym}$

[a] Parentheses denote relative intensities in the Raman effect.
[b] s = strong, m =medium, sh = shoulder, br = broad.
[c] Not observed.

Table 20. Selected features and their assignments in the vibrational spectra of **19**–**21**.[a,b]

Me$_3$Ge[SCO$_2$Me], **19**		Me$_3$Ge[SCO$_2$(*i*-Pr)], **20**		Me$_3$Ge[SCO$_2$(*n*-Pr)], **21**		
IR	Raman	IR	Raman	IR	Raman	Assignment
1694 vs	1687 (5)	1694 vs	1688 (5)	1691 vs	1688 (2)	$\nu(SCO_2C)_a$
1145 vs	1145 (5)	1134 vs	1140 (3)	1132 vs	n.o.	$\nu(SCO_2C)_b$
1067 s,sh	1097 (5)	1090 s	1091 (2)	1066 s,sh	1088 (3)	$\nu(SCO_2C)_c$
820 s,sh	848 (10)	835 s	840 (5)	832 s	841 (5)	$\pi(SCO_2)$
676 s	n.o.[c]	678 s	n.o.	675 s	n.o.	$\nu(SCO_2C)_d$
627 s	611 (30)	617 ms	612 (40)	613 s	610 (35)	$\nu(Ge\text{-}C)_{asym}$
587 s	569 (100)	575 s	570 (100)	570 ms	569 (100)	$\nu(Ge\text{-}C)_{sym}$
441 s	437 (10)	434 s	437 (2)	419 ms	421 (5)	ν(Ge-S)

[a] Parentheses denote relative intensities in the Raman effect.
[b] s = strong, m = medium, sh = shoulder, br = broad.
[c] Not observed.

$Me_2GeCl[S_2CNEt_2]$ where ν(Ge–Cl) was assigned at 293 cm^{-1} (8). Similarly, ν(Ge–Br), is at ca. 224 cm^{-1} in all $Ph_2GeBr[S_2CSR]$, **9**–**12**, compared to ca. 315 cm^{-1} Ph_2GeBr_2. This weakening of the Ge—X bond by the trithiocarbonate group may contribute to the difficulty of isolating the mixed $Me_2GeX[S_2CSR]$ species. A weak Ge—X bond, accompanied by less stereochemical hindrance to an incoming group with Me rather than Ph groups attached to germanium, could result in partially substituted compounds acting as reactive intermediates that could also undergo rapid exchange to the bis substituted species and dihalodimethylgermane.

Distinctive features in the infrared and Raman spectra and their assignments are given for $Ph_3Ge[SCO_2R]$, **13**–**15**, $Ph_2Ge[SCO_2R]_2$, **16**–**18**, and $Me_3Ge[SCO_2R]$, **19**–**21**, in Tables 18–20. The assignments are based on the same factors described for the trithiocarbonates along with trends involving related dithiocarbonate species. A strong band attributable to the C═O stretching vibration, ν(C═O), which is observed at ca. 1620 cm^{-1} in the $NaSCO_2R$ salts, is shifted to higher wave number (1690–1703 cm^{-1}) in all nine compounds. This supports the presence of an essentially monodentate monothiocarbonate ligand with a very strong terminal C═O bond. The O atoms of the SCO_2C group should give rise to two intense peaks in the infrared spectra, in addition to the one at 1690–1703 cm^{-1}, and two such peaks, which are presumably primarily attributable to ν(SC–O) and ν(SCO–C), are seen in the region 1188–1066 cm^{-1} for **13**–**21,** designated $\nu(SCO_2C)_b$ and $\nu(SCO_2C)_c$, respectively. These assignments are entirely consistent with the X-ray structures of compounds **13, 14**, and **16**. Two distinctive strong peaks are also seen at ca. 840 and 670 cm^{-1}. The former can be assigned to the out-of-plane bend, $\pi(SCO_2)$, which is assigned at 830–873 cm^{-1} for $\pi(CO_3)$ in carbonate salts, suggesting similar π-electron delocalization in these planar groups. The fourth stretching vibration, $\nu(SCO_2C)_d$, presumably primarily ν(GeS–C), is assigned to 670–678 cm^{-1}, which is similar to general assignments of C—S single bonds and to the assignments reported for the corresponding dithiocarbonates.

The Ge–S vibrational modes are readily assigned within 440–400 cm^{-1} for **13**–**21** in similar positions to those in the dithiocarbamates (4–6) and Me_3GeSR (30), but at slightly higher wave number compared to those of the trithiocarbonates. This is consistent with the greater tendency for the trithiocarbonates to form anisobidentate links leading to slightly weaker Ge—S primary bonds. The Ge—S bond lengths in **13, 14**, and **16** are slightly shorter than those of $Me_2Ge[S_2CSEt]_2$, **1**, and $Ph_2Ge[S_2CS(i\text{-}Pr)]_2$.

The crystal structure of $Me_2Ge[S_2CSEt]_2$, 1

Dimethylbis(*S*-ethyl trithiocarbonato)germane, **1**, crystallizes in the space group $P2_1/m$. The ORTEP diagram in Fig. 1(*a*) illustrates, along with Table 6, that the immediate environment about germanium is that of a distorted tetrahedron. The S-Ge-C angles have an average value of 108.8(10)° compared with 111.8(17)° for $Ph_2Ge[S_2CS(i\text{-}Pr)]_2$ (15). By contrast, the C-Ge-C angles are very much larger than the regular tetrahedral angle: 128.8(6)° in **1** compared with 118.1(3)° in $Ph_2Ge[S_2CS(i\text{-}Pr)]_2$. This opening up of the C-Ge-C angle in $Me_2Ge[S_2CSEt]_2$ was predicted from its vibrational spectrum. The average Ge—C bond length of 1.93(1) Å is typical for R_2GeL_2 or R_3GeL species, where L is a sulfur-bonding moiety, being similar to those in $Ph_2Ge[S_2CS(i\text{-}Pr)]_2$, $Ph_2Ge[S_2CO(i\text{-}Pr)]_2$ (12), $Me_2Ge[S_2CNMe_2]_2$ (6), $Me_2GeCl[S_2CNMe_2]$ (5), and even in $Ph_3GeSC_6H_4(t\text{-}Bu)$ (31).

Fig. 1. ORTEP plots of the molecule $Me_2Ge[S_2CSEt]_2$ (**1**) illustrating (*a*) the tetrahedral environment about germanium, (*b*) the pendant sulfur atoms acting as weak donors, and (*c*) the planarity of all non-hydrogen atoms except the carbon atoms of the ethyl groups. The atoms are drawn with 30% probability ellipsoids. Hydrogen atoms omitted for clarity in (*a*) and (*b*).

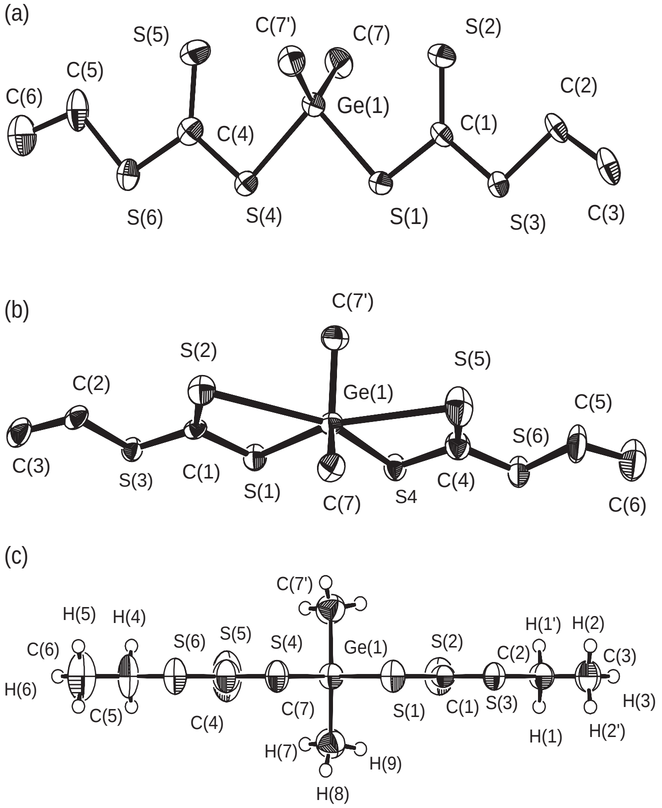

The closing down of the S-Ge-S angles to 90.0(1)° in **1** is similar to that observed in the dithiocarbamate analogues, $Ph_2Ge[S_2CNEt_2]_2$ and $Me_2Ge[S_2CNMe_2]_2$, where the S-Ge-S angles are 84.4(1)° and 87.0(1)°, respectively. These smaller angles are associated with the fact that a terminal sulfur (C═S) atom is oriented toward the germanium center (see Fig. 1) at Ge—S distances of 3.051(5) and 3.246(5) Å for $Me_2Ge[S_2CSEt]_2$, 3.078(2) and 3.158(2) Å for $Me_2Ge[S_2CNMe_2]_2$, 3.224(5) and 3.304(5) Å for $Ph_2Ge[S_2CS(i\text{-}Pr)]_2$, and 3.183(1) Å for $Ph_2Ge[S_2CNEt_2]_2$. By contrast, in the analogous dithiocarbonate, $Ph_2Ge[S_2CO(i\text{-}Pr)]_2$, where the terminal sulfur atom is oriented away from the germanium center (with Ge—S = 4.753(4) Å), the S-Ge-S angle is much larger at 103.2(1)° (12). Whether distances in the range of 3.05–3.3 Å, which are considerably less than the sum of the van der Waals radii of 3.75 Å, are sufficiently short to be considered as partial bonds may be questioned, but there is a relationship between these Ge—S nonbonding or anisobonding distances and the closing down of the S-Ge-S angle from the regular tetrahedral angle when the sulfur atom is oriented toward, rather than away from, germanium.

The average Ge—S bond length (2.295(1) Å) in **1** is longer than in the analogous dithiocarbonate, $Ph_2Ge[S_2CO(i\text{-}Pr)]_2$

(2.252(3) Å) in which there are no Ge—S secondary interactions (15). However, it is similar to those in $Ph_2Ge[S_2CNEt_2]_2$, $Me_2Ge[S_2CNMe_2]_2$, and other germanium dithiocarbamates where there is the same probability of the presence of secondary bonding (6, 14). In view of the similarities noted in the spectra of the trithiocarbonates, all of these *S*-alkyl trithiocarbonate derivatives probably have the same weak anisobidentate bonding as indicated by the molecular structures of $Me_2Ge[S_2CSEt]_2$, **1**, and $Ph_2Ge[S_2CS(i\text{-}Pr)]_2$ (15). The C=S bonds in **1**, which average 1.63(8) Å, are very slightly longer than those in $Ph_2Ge[S_2CO(i\text{-}Pr)]_2$, 1.61(1) Å, which is again consistent with the presence of weak secondary interactions leading to the orientation of the terminal C=S rather than the CSR moiety toward the germanium centre. The average bite angle of 62.4(7)° in $Ph_2Ge[S_2CS(i\text{-}Pr)]_2$ is essentially the same as that in $Ph_2Ge[S_2CNEt_2]_2$, where anisobidentate linkages appear to give a better overall description of the bonding of dithiocarbamates to germanium (14). There is an even larger bite angle of 65.8(1)° in **1**, which suggests an even stronger anisobidentate bond as implied by the inclusion of Ge(1)—S(2) and Ge(1)—S(4) bonds in Fig. 1(*b*).

The S—CR bonds in the trithiocarbonate groups at 1.82(2) Å are essentially as expected from the sum of the covalent radii of S and C, whereas the average length of C—SGe and C—SR bonds is 1.74(2) Å, and that of the "terminal" C=S bond is 1.63(1) Å, indicating that π-electron density delocalization is not significantly extended beyond the planar groups. Nevertheless, all of the non-hydrogen atoms in both trithiocarbonate groups are coplanar, as required by the mirror plane, and the relationship between the groups is well illustrated by Fig. 1(*c*).

The crystal structures of $Ph_3Ge[SCO_2Me]$, 13, $Ph_3Ge[SCO_2(i\text{-}Pr)].0.5CH_2Cl_2$, 14, and $Ph_2Ge[SCO_2Me]_2$, 16

Triphenyl(*O*-methyl monothiocarbonato)germane, **13**, and triphenyl(*O*-isopropyl monothio-carbonato)germane, **14**, both crystallize in the space group $P\bar{1}$ (No. 2), the latter with dichloromethane in the lattice. The ORTEP diagrams in Figs. 2 and 3 illustrate, along with Tables 7 and 8, that the immediate environment about germanium in both molecules is that of a distorted tetrahedron. The average values of the C-Ge-C angles are 110.8(4)° in **13** and 111.6(16)° for the two independent molecules in **14**, while those of the S-Ge-C angles are 108(6)° in **13** and 107(5)° in **14**. It is immediately obvious that the variation in the S-Ge-C angles is larger than for the C-Ge-C angle, which arises because one S-Ge-C angle is considerably smaller (100.4(3)° in **13** and 99.4(3)° in **14**) than the other two (111.8(15)° in **13** and 110.7(27)° in **14**). All of these values are close to those found for the analogous dithiocarbonates, $Ph_3Ge[S_2COMe]$ and $Ph_3Ge[S_2CO(i\text{-}Pr)]$. The similarity extends to dithiophospates, such as $Ph_3Ge[S_2P(OMe)_2]$, where one S-Ge-C angle is again significantly smaller than the other two (4). In the dithiocarbonates and dithiophosphates, an alkoxy group is oriented towards germanium in preference to a terminal sulfur atom, whereas in **13** and **14** the alkoxy group is oriented away from germanium and the terminal oxygen atom toward germanium. Possibly, the slightly smaller range in the S-Ge-C angles in the monothiocarbonates reflects the fact that the less bulky terminal oxygen atom is more readily accommodated.

Fig. 2. ORTEP plot of the molecule $Ph_3Ge[SCO_2Me]$ (**13**). The atoms are drawn with 30% probability ellipsoids. Hydrogen atoms omitted for clarity.

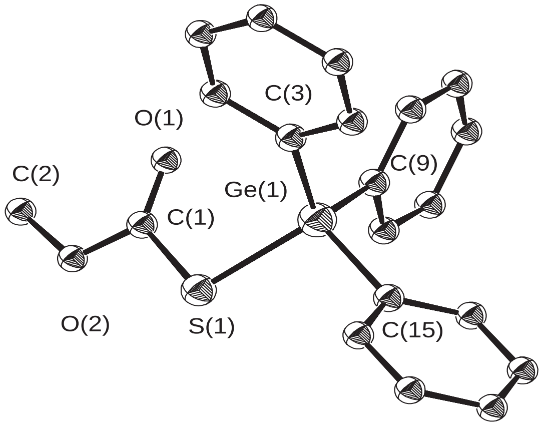

The Ge—C distances, which range from 1.931(9) to 1.950(9) Å in **13** and 1.93(1) to 1.94(1) Å in **14**, are comparable with those found in the analogous trithiocarbonates and related species as described above, and cover the same range as in the dithiophosphate, $Ph_3Ge[S_2P(OMe)_2]$, 1.930(5)–1.950(5) Å. The Ge—S bond length of 2.254(3) Å in both **13** and **14** is bracketed by those reported for the dithiocarbonates, $Ph_3Ge[S_2COMe]$ (2.249(4) Å) and $Ph_3Ge[S_2CO(i\text{-}Pr)]$ (2.272(2) Å), and slightly shorter than in the dithiophosphate, $Ph_3Ge[S_2P(OMe)_2]$ (2.285(1) Å).

As expected, the terminal C=O bond lengths of 1.19(1) and 1.20(5) Å in **13** and **14**, respectively, are much shorter than the other C—O bonds. They are also close to the expected value for a C=O double bond. The SC—O bonds, in turn, are significantly shorter than the SCO—C bonds, being similar to those reported for the two analogous dithiocarbonates (avg. 1.34(1) and 1.45(1) Å, respectively), which is consistent with the π-bond character not extending significantly beyond the planar SCO_2 core.

The terminal O atom is oriented towards germanium, with the Ge—O distance being 3.112(7) and 3.12(2) Å in **13** and **14**, respectively, which is similar to the Ge—S distances in trithiocarbonates. Thus, the intramolecular interactions, if any, must be extremely weak. However, as mentioned above, the orientations of the ligand in the dithiocarbonates and $Ph_3Ge[S_2P(OMe)_2]$ are both such as to place the (OR) groups, rather than the terminal sulfur atoms, closer to the germanium center and the Ge—OR distances in $Ph_3Ge[S_2COMe]$ (2.98(2) Å) and $Ph_3Ge[S_2CO(i\text{-}Pr)]$ (3.115(4) Å), are similar to the Ge—O(terminal) distances in **13** and **14**.

Diphenylbis(O-methyl monothiocarbonato)germane, $Ph_2Ge[SCO_2Me]_2$, **16**, crystallizes in the space group *Cc* (No. 9). The ORTEP diagram (Fig. 4) and Table 9 confirm that the immediate environment about germanium is again the expected distorted tetrahedron. The S-Ge-S angle of 93.3(7)° and C-Ge-C angle of 117.85(7)° are very close to those in the analogous dithiocarbonates, $Ph_2Ge[S_2COMe]_2$, where the corresponding angles are 93.4(2)° and 117.1(3)°) (11). The distortion from the regular tetrahedral angle is greater than was found for $Ph_2Ge[S_2CO(i\text{-}Pr)]_2$ (12), where the corresponding angles are 103.2(1)° and 115.6(3)°, but less than that found for the trithiocarbonate, $Ph_2Ge[S_2CS(i\text{-}Pr)]_2$, described earlier (15), where the corresponding angles are 87.3(2)° and 118.1(3)° respec-

Fig. 3. ORTEP plot of the molecule $Ph_3Ge[SCO_2(i\text{-}Pr)]$ (**14**) showing both molecules in the asymmetric unit as well as the CH_2Cl_2 trapped in the lattice. The atoms are drawn with 30% probability ellipsoids. Hydrogen atoms omitted for clarity except for those in dichloromethane.

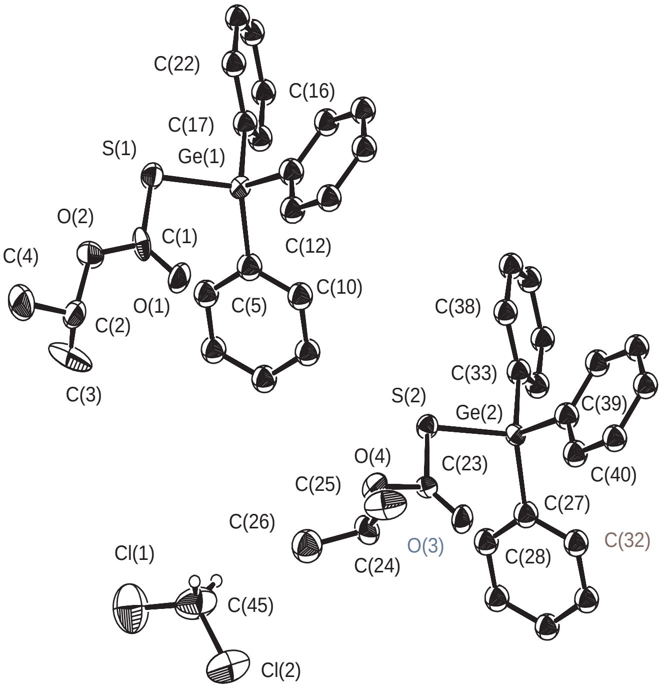

tively, or $Me_2Ge[S_2CSEt]_2$, **1**, with angles of 90.0(1)° and 128.6(6)°, respectively. The S-Ge-S angle in **16** is considerably wider than the 84.4° in $Ph_2Ge[S_2CNEt_2]_2$ (8), where the ligand was assumed to be anisobidentate.

The Ge—C bond length of 1.928(5) Å in **16** is again very similar to those reported for **13** and **14**, as well for trithiocarbonates including **1**, and the other S-linked groups mentioned earlier. The average Ge—S bond length in **16** of 2.258(4) Å brackets those observed in $Ph_2Ge[S_2COMe]_2$ (2.262(3) Å) and $Ph_2Ge[S_2CO(i\text{-}Pr)]_2$ (2.252(1) Å) and is slightly shorter than those found for the dithiocarbamate, $Ph_2Ge[S_2CNEt_2]_2$ (2.277(2) Å) and the trithiocarbonate, $Ph_2Ge[S_2CS(i\text{-}Pr)]_2$ (2.280(5) Å). In general, the bis compounds appear to have slightly longer Ge—S bonds than those containing only one thio ligand as in **13** and **14.**

The GeS—C average bond length in **16** of 1.77(1) Å is not significantly different from those in **13** and **14**, and is typical of values observed in $Ph_2Ge[S_2COMe]_2$, $Ph_2Ge[S_2CO(i\text{-}Pr)]_2$, and $Ph_2Ge[S_2CNEt_2]_2$ (1.76(1) Å), as well as for $Ph_2Ge[S_2CS(i\text{-}Pr)]_2$ (1.745(6) Å). The distances between germanium and the terminal O atom of 3.00(1) and 3.07(1) Å are similar to those in **13** and **14**, as are the S-Ge—O bite angles, which range from 57.3(3)° to 62.9(1)°, again indicating that if there is any secondary interaction between germanium and the terminal O atom, it must be very weak. The bond lengths and angles within the SCO_2C group of **16** are essentially the same as in **13** and **14**. The angles in the planar core do indeed add up to 360°, with average values in **16** being O═C-S (125.8(13)°), O═C-O (125.8(17)°), and S-C-O (108.5(13)°) compared with O═C-S (125.0(14)°), O═C-O (125.7(6)°, and S-C-O (109.3(16)° for **13** and **14**. The much larger angles involving the terminal C═O bond reflect the fact that this is the bond most strongly involved in the delocalized π-bonding. The average value of the C-O-C angle in all three molecules is 116(1)°, which is consistent with much less π-bond character in C—O bonds involved in the C-O-C link than in the SCO_2 core. The Ge-S-C angles, which ranged from 96.5(7)° to 100.5(6)°, are somewhat smaller, but essentially very similar to the corresponding angles in $Ph_2Ge[S_2COMe]_2$, 102.7(5)°, $Ph_2Ge[S_2CO(i\text{-}Pr)]_2$, 105.0(3)°, $Ph_2Ge[S_2CNEt_2]_2$, 102.1(1)°, as well as in $Ph_2Ge[S_2CS(i\text{-}Pr)]_2$, 101(1)°, indicating little or no change in the nature of this link regardless of the thio derivative attached.

Fig. 4. ORTEP plots of the molecule $Ph_2Ge[SCO_2Me]_2$ (**16**) showing different views of the two molecules in the asymmetric unit. The atoms are drawn with 30% probability ellipsoids. Hydrogen atoms omitted for clarity except for those in dichloromethane.

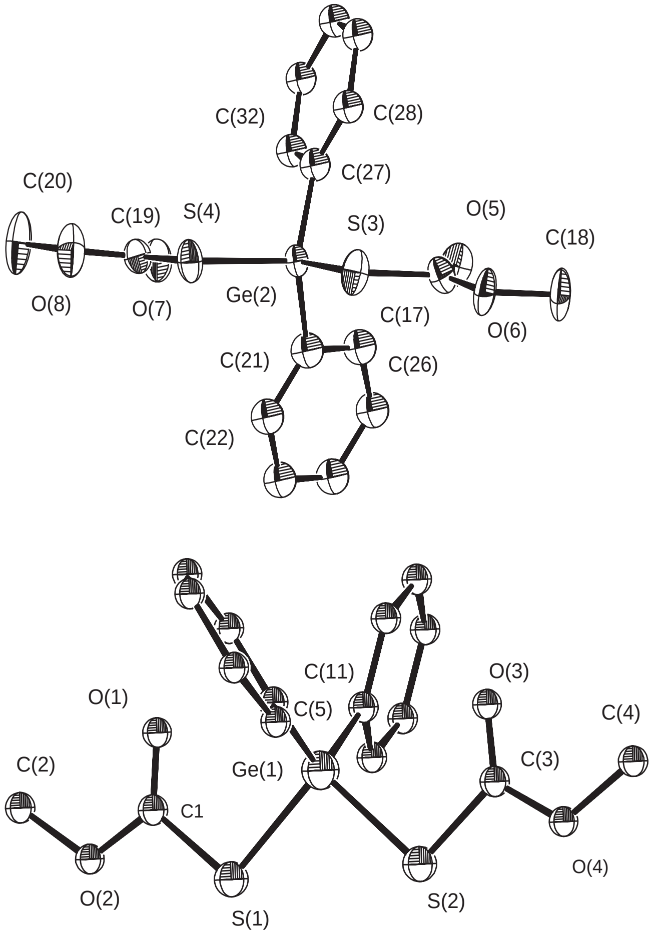

Concluding comments

Previous studies of organogermanium dithiocarbonates gave a wide variety of relatively stable derivatives, some of which were tested for suitability as oil additives. Given the paucity of work on any main group monothiocarbonates, it is somewhat surprising that organogermanium monothiocarbonates have proven to be relatively easy to prepare and characterize fully by spectroscopic methods as well as by X-ray crystallography. However, the organogermanium trithiocarbonates all readily eliminate CS_2 regardless of the nature of the organo groups or the number of groups attached to germanium. By contrast, the only sign of reductive elimination in the monothiocarbonates is the presence of the COS^+ ion in some of their mass spectra. The interpretation of the NMR and vibrational spectra is entirely consistent, with the structures found in the solid state being essentially maintained in solution. Thus, like the dithiocarbonates, there is an essentially monodentate link through sulfur. However, in all cases in the solid state, there is apparently a weak interaction with the "terminal" sulfur atom (for tri- and dithiocarbonates) and possibly even with the "terminal" oxygen atom (for monothiocarbonates) as these atoms are oriented toward the germanium center at distances well inside that of the sum of the van der Waals radii, particularly for Ge—S. In related tellurium species, we found that on occasion, as in $Ph_2Te[SCO_2(i\text{-}Pr)]_2$, one of the OR groups was oriented toward tellurium and the pendant oxygen was possibly involved in a weak link to an adjacent tellurium center, creating a weakly bonded extended structure. There was no indication of similar behavior with germanium.

Acknowledgement

We wish to thank the Natural Sciences and Engineering Research Council of Canada for financial support.

References

1. D. Coucouvanis, S.J. Lippard, and J.A. Zubieta. J. Am. Chem. Soc. **92**, 3342 (1970).
2. J.W. Andrews, D. Coucouvanis, and J.P. Fackler, Jr. Inorg. Chem. **3**, 4932 (1972).
3. D. Coucouvanis. Prog. Inorg. Chem. **26**, 310 (1979).
4. R.K. Chadha, J.E. Drake, and A.B. Sarkar. Inorg. Chem. **24**, 3156 (1985).
5. R.K. Chadha, J.E. Drake, and A.B. Sarkar. Inorg. Chem. **23**, 4769 (1984).
6. R.K. Chadha, J.E. Drake, and A.B. Sarkar. Inorg. Chem. **25**, 2201 (1986).
7. R.K. Chadha, J.E. Drake, and A.B. Sarkar. Inorg. Chem. **26**, 2885 (1987).
8. R.K. Chadha, J.E. Drake, and A.B. Sarkar. Inorg. Chim. Acta, **143**, 31 (1988).
9. J.E. Drake, A.G. Mislankar, and R. Ratnani. Can. J. Chem. **72**, 830 (1994).
10. J.E. Drake, L.N Khasrou, A.G. Mislankar, R. Ratnani, and J. Yang. Can. J. Chem. **73**, 915 (1995).
11. J.E. Drake, A.B. Sarkar, and M.L.Y. Wong. Inorg. Chem. **29**, 785 (1990).
12. J.E. Drake, A.B. Sarkar, and M.L.Y. Wong. Inorg. Chem. **30**, 2174 (1991).
13. J.E. Drake, A.G. Mislankar, and J. Yang. Inorg. Chem. **31**, 5543 (1992).
14. J.E. Drake, A.G. Mislankar, and J. Yang. Inorg. Chim. Acta, **211**, 37 (1993).
15. J.E. Drake and J. Yang. Inorg. Chem. **33**, 854 (1993).
16. K.K. Pandey and H.L. Wingan. Rev. Inorg. Chem. **6**, 71 (1984).
17. S. Datta and H.L. Agarwala. Indian J. Chem. **20A**, 1190 (1981).
18. T.V. Ashworth, M. Nolte, and E.J. Singleton. J. Organomet. Chem. **121**, C57 (1975).
19. T.R. Gaffney and J.A. Ibers. Inorg. Chem. **21**, 2860 (1982).
20. N. Sonoda and T. Tanaja. Inorg. Chim. Acta, **12**, 261 (1975).
21. C. Bender. Bull. Chem. Soc. **12**, 256 (1869).
22. J.E. Drake, A.G. Mislankar, R. Ratnani, and J. Yang. Can. J. Chem. **74**, 1968 (1996).
23. C.C. Dewitt and E.E. Roper. J. Am. Chem. Soc. **54**, 444 (1932).
24. G.M. Sheldrick. Acta Crystallogr. Sect.A: Found. Crystallogr. **A46**, 467 (1990).
25. TEXSAN-TEXRAY structure analysis package. Molecular Structure Corp., The Woodlands, Tex. 1985 and 1992.
26. W. Metlesics and H. Zeiss. J. Am. Chem. Soc. **82**, 3321 (1960).
27. D.H Wiffen. J. Chem. Soc. 3350 (1956).
28. J.D. Ross. Inorganic IR and Raman spectra. McGraw–Hill, London. 1972. p 160.
29. J.E. Griffiths. Spectrochim. Acta, **20**, 1335 (1964).
30. J.E. Drake, H.E. Henderson, and L.N. Khasrou. Spectrochim. Acta, **38A**, 31 (1982).
31. M.E. Cradwick, R.D. Taylor, and J.L. Wardell. J. Organomet. Chem. **66**, 43 (1974).